Table 2. Correlations between human endoplasmic reticulum oxidoreductin 1-α (hERO1-α) status and other clinicopathological factors in patients with breast cancer (n = 71)

	hERO1-α (+)	hERO1-α (−)	P-value
Mean age, years (range)	55.4 ± 13.5	58.8 ± 12.6	0.2764
Histological type			
Papillotubular	16	12	
Solid-tubular	4	3	
Scirrhous	9	16	
Others	4	7	
pT			
pT1 (≤2.0 cm)	10	12	0.8376
pT2 (2.0 ≤ 5.0 cm)	19	23	
pT3 (>5.0 cm)	4	3	
pN			
pN (−)	13	11	0.3535
pN (+)	20	27	
ER, PgR, HER2 status			
ER (+) or PgR (+) and HER2 (−)	14	28	0.0210
ER (+) or PgR (+) and HER2 (+)	5	5	
ER (−) and PgR (−) and HER2 (+)	9	2	
ER (−) and PgR (−) and HER2 (−)	5	3	
Nuclear grade (NG)			
NG1	9	13	0.0010
NG2	7	20	
NG3	17	5	
Ly			
Ly (+)	19	16	0.1926
Ly (−)	14	22	
V			
V (+)	6	5	0.5600
V (−)	27	33	

ER, estrogen receptor; HER2, human epidermal growth factor receptor type 2; Ly, lymph node invasion; PgR, progesterone receptor; V, vascular invasion.

hERO1-α, indicating endoplasmic reticulum localization, was found in 33 cases (46.5%) of the 71 patients with breast cancer (Fig. 6c,d). Correlations of hERO1-α (+) and hERO1-α (−) with clinicopathological factors are shown in Table 2. Human ERO1-α (+) type was positively correlated with ER (−) (P = 0.021) and high nuclear grade (P = 0.001). These results suggest that hERO1-α (+) type has a more aggressive phenotype than that of hERO1-α (−) type in breast cancer. No association of hERO1-α (+) type with age, histology, tumor size, or lymph node metastasis was found.

In univariate survival analysis, patients with hERO1-α (+) cancer had significantly shorter disease-free survival

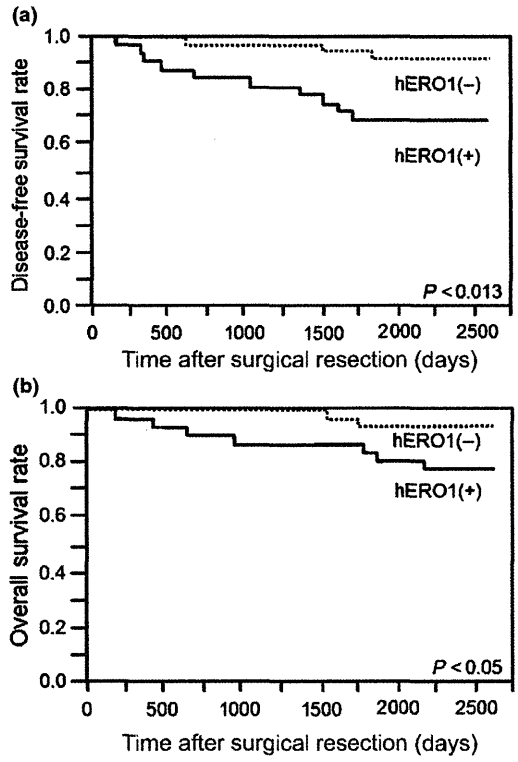

Fig. 7. Kaplan–Meier analysis of disease-free survival (a) and overall survival (b) for human endoplasmic reticulum oxidoreductin 1-α (hERO1-α) expression in 71 cases of invasive breast carcinoma.

(P = 0.01) (Fig. 7a) and overall survival (P = 0.04) (Fig. 7b) than did patients with hERO1-α (−) cancer. In multivariate analysis of disease-free survival by Cox regression analysis, expression of hERO1-α was the only independent prognostic factor (Table 3).

Importantly, we observed the intratumoral heterogeneity of hERO1-α expression, ranging from negative to strong in intensity by immunohistochemistry (Fig. 6c). It has been shown that the hypoxic areas were frequently observed within cancer tissues. As the expression of hERO1-α is induced under hypoxia (Fig. 1d), we assumed that cancer cells residing within hypoxic areas showed augmented expression of hERO1-α. Thus, the heterogeneity of hERO1-α expression seems to be attributed to the oxygen and blood supply. The relationship between hERO1-α and vessel distribution needs to be investigated.

Table 3. Univariate and multivariate survival analyses in breast cancer patients (n = 71)

	Univariate analysis			Multivariate analysis		
	Relative risk	95% CI	P-value	Relative risk	95% CI	P-value
T (≥2 cm, <2 cm)	0.97	0.30–4.32	0.9602	0.83	0.19–3.34	0.7988
NG (1 + 2, 3)	0.47	0.16–1.47	0.1862	0.80	0.22–3.04	0.7407
LN meta (+, −)	0.87	0.24–2.68	0.8193	0.83	0.19–3.35	0.7988
Ly (+, −)	1.24	0.41–3.85	0.6980	1.44	0.35–5.66	0.6020
V (+, −)	0.44	0.02–2.21	0.3694	0.33	0.02–2.10	0.2640
hERO1-α (+, −)	4.46	1.36–19.90	0.0122	4.13	1.10–20.08	0.0352

CI, confidence interval; hERO1-α, human endoplasmic reticulum oxidoreduction 1-α; LN meta, lymph node metastasis; Ly, lymph node invasion; NG, nuclear grade; V, vascular invasion.

Discussion

In this study, we showed that ERO1-α was overexpressed in the highly metastatic breast cancer cell line 4T1 and in patients with breast cancer recurrence. Depletion of ERO1-α by shRNA in 4T1 cells inhibited *in vivo* tumor growth as well as lung metastasis, suggesting that ERO1-α plays a pivotal role in tumor progression and metastasis. Moreover, a positive correlation was found between hERO1-α expression and recurrence in breast cancer patients, which is mainly caused by dissociation of tumor cells from the primary tumor and dissemination into other sites during tumor progression. Thus, these results suggested that ERO1-α (+) tumor cells were more likely to invade into the stroma and vasculature and then metastasize to remote organs, as indicated by the results of knockdown of ERO1-α. We also found an association between hERO1-α expression and high levels of nuclear grade in clinical specimens, indicating high proliferative activity of tumor cells. Moreover, we showed that ERO1-α plays a pivotal role in VEGF production through disulfide bond formation by PDI within VEGF protein, suggesting that ERO1-α affects tumor growth through angiogenic signaling pathways.[11] Most notably, the fact that the expression of ERO1-α is induced under hypoxic conditions seems to be beneficial to tumor cells to overcome such stressful conditions through production of VEGF-A and other angiogenic factors. These results suggest that ERO1-α plays a pivotal role in survival of cancer cells at the tumor origin against hypoxic conditions, as well as accelerating metastasis through production of angiogenic factors including VEGF-A through disulfide bond formation. In fact, hERO1-α (+) breast cancer patients showed a higher recurrence rate and more dismal outcome after surgery. All of these findings indicate that the expression of hERO1-α is significantly related to aggressive phenotype of breast cancer; hERO1-α can be a new prognostic marker for breast cancer after surgery. However, it should be determined how ERO1-α expression is regulated under hypoxia and within tumor cells and, more importantly, the precise mechanism for tumor cell growth should be elucidated.

Until now, there has been no ideal tumor marker with prognostic value. The predictive significance of hERO1-α in breast cancer could help clinicians identify patients at high risk for recurrence, and enable clinicians to carry out rational adjuvant therapy after surgery. Taken together, our results indicate that hERO1-α may be a suitable prognostic marker for breast cancer.

In addition, the potential for targeting hERO1-α in cancer therapy seems promising, as hERO1-α is overexpressed in many human cancers but is barely detectable in normal tissues. Thus, cancer therapy targeting hERO1-α activity may be a promising strategy for treatment of various types of cancer.

Acknowledgments

This work was supported in part by a program for developing the supporting system for upgrading education and research from the Ministry of Education, Culture, Sports, Science and Technology of Japan.

Disclosure Statement

The authors have no conflict of interest.

References

1 Lunt SJ, Chaudary N, Hill RP. The tumor microenvironment and metastatic disease. *Clin Exp Metastasis* 2009; **26**: 19–34.
2 Chaudary N, Hill RP. Hypoxia and metastasis in breast cancer. *Breast Dis* 2006; **26**: 55–64.
3 Milosevic M, Chung P, Parker C *et al.* Androgen withdrawal in patients reduces prostate cancer hypoxia: implications for disease progression and radiation response. *Cancer Res* 2007; **67**: 6022–5.
4 Milosevic M, Warde P, Menard C *et al.* Tumor hypoxia predicts biochemical failure following radiotherapy for clinically localized prostate cancer. *Clin Cancer Res* 2012; **18**: 2108–14.
5 Benham AM, Cabibbo A, Fassio A, Bulleid N, Sitia R, Braakman I. The CXXCXXC motif determines the folding, structure and stability of human ERO1-Lalpha. *EMBO J* 2000; **19**: 4493–502.
6 Gess B, Hofbauer KH, Wenger RH, Lohaus C, Meyer HE, Kurtz A. The cellular oxygen tension regulates expression of the endoplasmic oxidoreductase ERO1-Lalpha. *Eur J Biochem* 2003; **270**: 2228–35.
7 Araki K, Nagata K. Functional in vitro analysis of the ERO1 protein and protein-disulfide isomerase pathway. *J Biol Chem* 2011; **286**: 32705–12.
8 Masui S, Vavassori S, Fagioli C, Sitia R, Inaba K. Molecular bases of cyclic and specific disulfide interchange between human ERO1alpha and PDI. *J Biol Chem* 2011; **286**: 16261–71.
9 Tavender TJ, Bulleid NJ. Molecular mechanisms regulating oxidative activity of the ERO1 family in the endoplasmic reticulum. *Antioxid Redox Signal* 2010; **13**: 1177–87.
10 Tanaka S, Uehara T, Nomura Y. Up-regulation of protein-disulfide isomerase in response to hypoxia/brain ischemia and its protective effect against apoptotic cell death. *J Biol Chem* 2000; **275**: 10388–93.
11 May D, Itin A, Gal O, Kalinski H, Feinstein E, Keshet E. ERO1-L alpha plays a key role in a HIF-1-mediated pathway to improve disulfide bond formation and VEGF secretion under hypoxia: implication for cancer. *Oncogene* 2005; **24**: 1011–20.
12 Qin C, Wilson C, Blancher C, Taylor M, Safe S, Harris AL. Association of ARNT splice variants with estrogen receptor-negative breast cancer, poor induction of vascular endothelial growth factor under hypoxia, and poor prognosis. *Clin Cancer Res* 2001; **7**: 818–23.
13 Schindl M, Schoppmann SF, Samonigg H *et al.* Overexpression of hypoxia-inducible factor 1alpha is associated with an unfavorable prognosis in lymph node-positive breast cancer. *Clin Cancer Res* 2002; **8**: 1831–7.
14 Potgens AJ, Lubsen NH, van Altena MC *et al.* Covalent dimerization of vascular permeability factor/vascular endothelial growth factor is essential for its biological activity. Evidence from Cys to Ser mutations. *J Biol Chem* 1994; **269**: 32879–85.
15 Claffey KP, Senger DR, Spiegelman BM. Structural requirements for dimerization, glycosylation, secretion, and biological function of VPF/VEGF. *Biochim Biophys Acta* 1995; **1246**: 1–9.
16 Muller YA, Li B, Christinger HW, Wells JA, Cunningham BC, de Vos AM. Vascular endothelial growth factor: crystal structure and functional mapping of the kinase domain receptor binding site. *Proc Natl Acad Sci U S A* 1997; **94**: 7192–7.
17 Frand AR, Kaiser CA. ERO1p oxidizes protein disulfide isomerase in a pathway for disulfide bond formation in the endoplasmic reticulum. *Mol Cell* 1999; **4**: 469–77.

doi: 10.1111/cas.12177

Carcinogenesis vol.34 no.6 pp.1232–1243, 2013
doi:10.1093/carcin/bgt057
Advance Access publication February 6, 2013

Protein kinase Cα inhibitor protects against downregulation of claudin-1 during epithelial–mesenchymal transition of pancreatic cancer

Daisuke Kyuno[1,2], Takashi Kojima[2,*], Hiroshi Yamaguchi[1], Tatsuya Ito[1], Yasutoshi Kimura[1], Masafumi Imamura[1], Akira Takasawa[2], Masaki Murata[2], Satoshi Tanaka[2], Koichi Hirata[1] and Norimasa Sawada[2]

[1]Department of Surgery and [2]Department of Pathology, Sapporo Medical University School of Medicine, Sapporo 060-8556, Japan

*To whom correspondence should be addressed. Tel: +81-11-611-2111 ext. 2701; Fax: +81-11-613-5665;
Email: ktakashi@sapmed.ac.jp

Protein kinase Cα (PKCα) is highly expressed in pancreatic cancer. However, the effects of PKCα on Snail and claudin-1, which play crucial roles in epithelial cell polarity during epithelial–mesenchymal transition (EMT), remain unclear. In this study, we investigated the mechanisms of regulation of Snail and claudin-1 *via* a PKCα signal pathway during EMT in pancreatic cancer cells and in normal human pancreatic duct epithelial cells (HPDEs). By immunostaining, overexpression of PKCα and downregulation of claudin-1 were observed in poorly differentiated human pancreatic cancer tissues and the pancreatic cancer cell line PANC-1. Treatment with the PKCα inhibitor Gö6976 transcriptionally decreased Snail and increased claudin-1 in PANC-1 cells. The PKCα inhibitor prevented upregulation of Snail and downregulation of claudin-1 during EMT induced by transforming growth factor-β1 (TGF-β1) treatment and under hypoxia in PANC-1 cells. The effects of the PKCα inhibitor were in part regulated *via* an extracellular signal-regulated kinase (ERK) signaling pathway. The PKCα inhibitor also prevented downregulation of the barrier function and fence function during EMT in well-differentiated pancreatic cancer cell line HPAC. In normal HPDEs, the PKCα inhibitor transcriptionally induced not only claudin-1 but also claudin-4, -7 and occludin without a change of Snail. Treatment with the PKCα inhibitor in normal HPDEs prevented downregulation of claudin-1 and occludin by TGF-β1 treatment and enhanced upregulation of claudin-1, -4, -7 and occludin under hypoxia. These findings suggest that PKCα regulates claudin-1 *via* Snail- and mitogen-activated protein kinase/ERK-dependent pathways during EMT in pancreatic cancer. Thus, PKCα inhibitors may be potential therapeutic agents against the malignancy of human pancreatic cancer cells.

Introduction

Pancreatic cancer, which has a strong invasive capacity with frequent metastasis and recurrence, is known to be one of the most malignant human diseases and its death rate has not decreased over the past few decades (1). Thus, there is an urgent need to develop novel diagnostic and therapeutic strategies to reduce the mortality of pancreatic cancer patients.

Protein kinase C (PKC) belongs to the family of serine-threonine kinases and regulates various cellular functions, including adhesion, secretion, proliferation, differentiation and apoptosis (2). At least 12 different isozymes of PKC are known and can be subdivided into three classes (classic or conventional, novel and atypical isozymes) according to their responsiveness to activators (3,4). Levels of PKCα, PKCβ1, PKCδ and PKCι are higher in pancreatic cancer, whereas that of PKCε is higher in normal tissue (5,6). In addition, PKCα is thought to be one of the biomarkers for diagnosis of cancers (7). In pancreatic cancer, tumorigenicity is directly related to PKCα expression as demonstrated by decreased survival when it is overexpressed (8). The increased level of PKCα is also associated with pancreatic cancer cell proliferation (9). PKCα is also one of the regulators and therapeutic targets in cancer (10).

Epithelial–mesenchymal transition (EMT) is closely related to carcinoma progression and acts as a major driver of morphogenesis and tumor progression (11). The activation of PKC is involved in EMT. The PKC activator 12-*O*-tetradecanoylphorbol 13-acetate (TPA) induces EMT in human prostate cancer cells and pancreatic cancer cell line HPAC (12,13). Expression of PKCα and PKCδ closely contributes to EMT in colon cancer cells (14,15). Snail, which is a transcription repressor that plays a central role in EMT, directly binds to E-boxes of the promoters of claudin/occludin genes, resulting in repression of their promoter activities and loss of epithelial cell polarity (16).

In several human cancers, including pancreatic cancer, some tight junction protein claudins are abnormally regulated and therefore promising molecular targets for diagnosis and therapy (17,18). Tight junctions are the most apical components of intercellular junctional complexes in epithelial and endothelial cells. They separate the apical and basolateral cell surface domains, maintaining cell polarity (termed the 'fence' function), and selectively control solute and water flow through the paracellular space (termed the 'barrier' function) (19–22). It is thought that loss of tight junction function in part leads to invasion and metastasis of cancer cells (23). In particular, claudin-1, which is expressed in various types of epithelial cells, plays an important role in epithelial cell polarity, cancer invasion and metastasis (24–28).

Tight junction proteins are regulated by various cytokines and growth factors *via* distinct signal transduction pathways including PKC (29,30). We previously found that, in pancreatic cancer cell line HPAC, tricellulin localized at tricellular tight junctions was in part regulated *via* PKCδ and PKCε pathways (31), and the expression of claudin-18 and localization of claudin-4 and occludin were in part regulated *via* a PKCα pathway (13,32,33). Furthermore, in normal human pancreatic duct epithelial cells (HPDEs), some tight junction proteins are regulated *via* PKCα and PKCδ (34). However, little is known about how PKCα regulates claudin-1 in pancreatic cancer cells and normal HPDEs.

In this study, overexpression of PKCα and downregulation of claudin-1 were observed in poorly differentiated human pancreatic cancer tissues and pancreatic cancer cell lines. Treatment with the PKCα inhibitor Gö6976 prevents upregulation of Snail and downregulation of claudin-1 during EMT induced by transforming growth factor-β1 (TGF-β1) treatment or under hypoxia in a pancreatic cancer cell line (28). Our findings suggest that PKCα inhibitors may be potential therapeutic agents against human pancreatic cancer cells.

Abbreviations: EMT, epithelial–mesenchymal transition; ERK, extracellular signal-regulated kinase; FBS, fetal bovine serum; HPDEs, human pancreatic duct epithelial cells; hTERT, telomerase reverse transcriptase; JNK, c-Jun N-terminal kinase; mRNA, messenger RNA; NF-κB, nuclear factor-kappaB; PI3K, phosphatidylinositol 3-kinase; PKC, protein kinase C; pMAPK, phospho-MAPK; pPKCα, phospho-PKCα; siRNA, small interference RNA; TER, transepithelial electrical resistance; TGF-β1, transforming growth factor-β1; TPA, 12-*O*-tetradecanoylphorbol 13-acetate.

Materials and methods

Reagents and inhibitors

Rabbit polyclonal anti-occludin, anti-claudin-1, anti-claudin-4, anti-claudin-7, anti-Snail and mouse monoclonal anti-occludin (OC-3F10) antibodies were obtained from Zymed Laboratories (San Francisco, CA). A rabbit polyclonal anti-actin antibody and a nuclear factor-kappaB (NF-κB) inhibitor (IMD-0354) were purchased from Sigma–Aldrich, (St Louis, MO). Rabbit polyclonal anti-Snail, anti-phospho-PKCα (pPKCα) and PKCα antibodies were obtained

from Cell Signaling (Beverly, MA). Alexa 488 (green)-conjugated anti-rabbit IgG and Alexa594 (red)-conjugated anti-mouse IgG antibodies were purchased from Molecular Probes (Eugene, OR). Inhibitors of panPKC (GF109203X), PKCα (Gö6976), mitogen-activated protein kinase (MAPK) (U0126), p38 MAPK (SB203580), phosphatidylinositol 3-kinase (PI3K) (LY294002) and c-Jun N-terminal kinase (JNK) (SP600125) were purchased from Calbiochem-Novabiochem Corporation (San Diego, CA). TGF-β1 was purchased from PeproTech EC (London, UK).

Immunohistochemical analysis

Immunohistochemical analysis was performed to evaluate the expression and distribution of PKCα and claudin-1 in normal pancreatic tissues, well-differentiated and poorly differentiated pancreatic cancer tissues. Deparaffinized tissue sections were immersed in 10 mM Tris–1 mM ethylenediaminetetraacetic acid buffer (pH 9.0) for staining of PKCα or 10 mM sodium citrate (pH 6.0) for staining of claudin-1 and boiled for antigen retrieval by microwave (95°C, 30 min). Endogenous peroxidase activity was blocked using 3% hydrogen peroxidase for 10 min. The sections were incubated with rabbit polyclonal PKCα and claudin-1 antibodies (1:100 dilution) overnight at 4°C. The sections were incubated with a Dako REAL™ EnVision™/HRP, Rabbit/Mouse (Dako REAL™ EnVision™ Detection System; Dako, code K5007) for 1 h at room temperature. After washing with phosphate-buffered saline, the labeled secondary antibody was visualized by adding Dako REAL™ Substrate Buffer (Dako REAL™ EnVision™ Detection System; Dako, code K5007) containing Dako REAL™ DAB + Chromogen (Dako REAL™ EnVision™ Detection System; Dako, code K5007). The sections were counterstained with hematoxylin.

Cultures of cell lines and treatment

Human pancreatic cancer cell lines PANC-1, HPAF-II, BXPC-3 and HPAC were purchased from American Type Culture Collection (Manassas, VA). PANC-1 and HPAC cells were maintained in Dulbecco's modified Eagle's medium (Sigma–Aldrich) supplemented with 10% dialyzed fetal bovine serum (FBS; Invitrogen, Carlsbad, CA). HPAF-II cells were maintained in Dulbecco's modified Eagle's medium containing 10% FBS and supplemented with 0.1 mM non-essential amino acids (Sigma–Aldrich) and 1 mM sodium pyruvate (Sigma–Aldrich). BXPC-3 cells were maintained in RPMI-1640 (Sigma–Aldrich) supplemented with 10% FBS. The media for all cell lines contained 100 U/ml penicillin, 100 μg/ml streptomycin and 2.5 μg/ml amphotericin-B. All cells were plated on 60 mm culture dishes (Corning Glass Works, Corning, NY) that were coated with rat tail collagen (500 μg of dried tendon/ml in 0.1% acetic acid) and incubated in a humidified 5% CO_2 incubator at 37°C.

PANC-1 and HPAC cells were treated with 0.01–2 μg/ml Gö6976 for 24 h or 100 ng/ml TGF-β1 for 24 and 48 h. PANC-1 cells were pretreated with 20 μM U0126, 10 μM SB203580, 10 μM LY294002, 10 μM GF109203X, 10 μM SP600125 and 0.1 μM IMD-0354 for 30 min before treatment with 1 μg/ml Gö6976 for 24 h and were pretreated with 1 μg/ml Gö6976 for 30 min before treatment with 100 ng/ml TGF-β1 for 24 h. The PANC-1 cells were incubated in a 2% CO_2:2% O_2 incubator balanced with nitrogen with or without 1 μg/ml Gö6976 for 24 h. HPAC cells were pretreated with 1 μg/ml Gö6976 for 30 min before treatment with 100 ng/ml TGF-β1 for 24 h.

For RNA interference studies, small interference RNA (siRNA) duplexes targeting the messenger RNA (mRNA) sequences of human Snail were purchased from Invitrogen. The sequences were as follows: siRNA-1 of Snail (sense 5′-CCUCGCUGCCAAUGCUCAUCUGGGA-3′), siRNA-2 of Snail (sense 5′-AGGCCAAGGAUCUCCAGGCUCGAAA-3′), siRNA of PKCα (sense 5′-CCGAGUGAAACUCACGGACUUCAAU-3′) and siRNA of PKCβ (sense 5′-GAGACCGGAUGAAACUGACCGAUUU-3′). A scrambled siRNA sequence (BLOCK-iT Alexa Fluor fluorescent; Invitrogen) was employed as control siRNA. One day before transfection, the PANC-1 cells were plated in medium without antibiotics such that they would be half confluent at the time of transfection. The cells were transfected with 100 nM siRNAs using Lipofectamine RNAiMAX (Invitrogen) as a carrier according to the manufacturer's instructions.

Isolation and culture of HPDEs

Human pancreatic tissues were obtained from patients with pancreatic or biliary tract diseases who underwent pancreatic resection in the Sapporo Medical University hospital. Informed consent was obtained from all patients, and the study was approved by the ethics committee of Sapporo Medical University.

The procedures for primary culture of HPDEs were as reported previously (31,32,34). Some primary cultured HPDEs were transfected with the catalytic component of telomerase, the human catalytic subunit of the telomerase reverse transcriptase (hTERT) gene as described previously (31,32,34). The hTERT-HPDEs were cultured in serum-free Bronchial Epithelial Cell Medium kit (Lonza Walkersville, Walkersville, MD) and incubated in a humidified, 5% CO_2:95% air incubator at 37°C. In this experiment, second and third passaged cells were used.

The hTERT-HPDEs were treated with 1 and 2 μg/ml Gö6976 for 24 h or 20 ng/ml TGF-β1 for 24 and 48 h. Some cells were pretreated with 20 μM U0126, 10 μM SB203580, 10 μM LY294002, 10 μM GF109203X, 10 μM SP600125 and 0.1 μM IMD-0354 for 30 min before treatment with 1 μg/ml Gö6976 for 24 h and some cells were pretreated with 1 μg/ml Gö6976 for 30 min before treatment with 20 ng/ml TGF-β1 for 24 h. The hTERT-HPDEs were incubated in a 2% CO_2:2% O_2 incubator balanced with nitrogen with or without 1 μg/ml Gö6976 for 24 h.

Western blot analysis

Western blot analysis was performed as described previously (31,32,34). The membranes were incubated with polyclonal anti-claudin-1, anti-claudin-4, anti-claudin-7, anti-occludin, anti-Snail, anti-pPKCα, anti-PKCα, anti-phospho-extracellular signal-regulated kinase (ERK1/2), anti-ERK1/2 and anti-actin antibodies (1:1000) for 1 h at room temperature. The membranes were incubated with horseradish peroxidase-conjugated anti-rabbit IgG (Dako A/S, Copenhagen, Denmark) at room temperature for 1 h. The immunoreactive bands were detected using an enhanced chemiluminescence western blotting analysis system (GE Healthcare, Little Chalfont, UK).

RNA isolation and real-time PCR analysis

Total RNA was extracted and purified using TRIzol (Invitrogen). One microgram of total RNA was reverse transcribed into complementary DNA using a mixture of oligo (deoxythymidine) and superscript II reverse transcriptase according to the manufacturer's recommendations (Invitrogen). Real-time PCR detection was performed using a TaqMan Gene Expression Assay kit with a StepOnePlus™ real-time PCR system (Applied Biosystems, Foster City, CA). The amount of 18S ribosomal RNA (Hs99999901) mRNA in each sample was used to standardize the quantity of the following mRNAs: claudin-1 (Hs00221623), claudin-4 (Hs00533616), claudin-7 (Hs00154575), occludin (Hs00170162) and Snail1 (Hs00195591). The relative mRNA expression levels between the control and treated samples were calculated by the difference of the threshold cycle (comparative C_T [$\Delta\Delta C_T$] method) and presented as the average of triplicate experiments with a 95% confidence interval.

Immunocytochemistry

The cells were grown on 35 mm glass-base dishes (Iwaki, Chiba, Japan) coated with rat tail collagen. They were fixed with cold acetone and ethanol (1:1) at 20°C for 10 min. After rinsing in phosphate-buffered saline, the sections and cells were incubated with polyclonal anti-claudin-1 and monoclonal anti-occludin antibodies (1:100) at room temperature for 1 h and then with Alexa Fluor 488 (green)-conjugated anti-rabbit IgG (1:200) and Alexa Fluor 594 (red)-conjugated anti-mouse IgG (1:200) at room temperature for 1 h. 4′,6-diamidino-2-phenylindole (Sigma–Aldrich) was used for counterstaining of nuclei in the cells. The specimens were examined using an epifluorescence microscope (Olympus, Tokyo, Japan).

Measurement of transepithelial electrical resistance

The cells were cultured to confluence on inner chambers of 12 mm Transwell 0.4 μm pore-size filters (Corning Life Science). Transepithelial electrical resistance (TER) was measured using an EVOM voltmeter with an ENDOHM-12 (World Precision Instruments, Sarasota, FL) on a heating plate (Fine, Tokyo, Japan) adjusted to 37°C. The values are expressed in standard units of ohms per square centimeter and presented as the mean ± SD of triplicate experiments. For calculation, the resistance of blank filters was subtracted from that of filters covered with cells.

Diffusion of BODIPY-sphingomyelin

For measurement of the tight junctional fence function, we used diffusion of BODIPY-sphingomyelin with some modification (28). The samples were analyzed by confocal laser scanning microscopy (LSM510; Carl Zeiss, Jena, Germany). All pictures shown were generated within the first 5 min of analysis.

Data analysis

Signals were quantified using Scion Image Beta 4.02 Win (Scion, Frederick, MD). Each set of results shown is representative of at least three separate experiments. Results are given as means ± standard error of the mean. Differences between groups were tested by analysis of variance followed by a *post hoc* test and an unpaired two-tailed Student's *t*-test.

Results

Expression and distribution of PKCα and claudin-1 in normal pancreatic ducts, well- and poorly differentiated pancreatic duct carcinomas

In this study, we examined the expression and distribution of PKCα and claudin-1 in normal pancreatic ducts, well- and poorly differentiated

pancreatic duct carcinomas (Figure 1). PKCα was detected in cytoplasm of both pancreatic duct carcinomas and the expression in poorly differentiated pancreatic duct carcinoma was stronger than in well-differentiated pancreatic duct carcinoma, whereas in normal pancreatic ducts, PKCα was not detected. Claudin-1 was localized at the cell membranes of normal pancreatic ducts and well-differentiated pancreatic carcinoma, whereas in poorly differentiated pancreatic carcinoma, it was weakly detected in cytoplasm.

Expression patterns of PKCα, Snail, claudin-1, -4, -7 and occludin in hTERT-HPDEs and human pancreatic cancer cell lines

To study the relationship between activation of PKCα and expression of tight junction proteins in human pancreatic cancer cells and normal pancreatic duct epithelial cells, we first investigated the expression patterns of pPKCα, panPKCα and claudin-1 in hTERT-HPDEs, which are models of normal pancreatic duct epithelial cells (34), and human pancreatic cancer cell lines HPAF-II and HPAC, which are models of well- or moderately differentiated pancreatic cancers and BXPC-3 and PANC-1, which are models of poorly differentiated pancreatic cancers (35). pPKCα and panPKCα were detected in all pancreatic cancer cell lines and were strongly expressed in PANC-1 cells, whereas in hTERT-HPDEs, they were not detected (Figure 1B). Snail, an EMT marker, was highly expressed only in PANC-1 cells (Figure 1B). Claudin-1, -4 and occludin were detected in all cell types, but at a low level in PANC-1 cells compared with other cancer cells, whereas claudin-7 was not detected in PANC-1 cells (Figure 1C). In the poorly differentiated pancreatic cancer cell line PANC-1, PKCα and Snail were upregulated and claudin-1 was downregulated.

PKCα inhibitor downregulates Snail and upregulates claudin-1 and occludin in PANC-1 cells

To investigate the effects of the PKCα inhibitor on the expression of Snail and tight junction proteins in the poorly differentiated pancreatic cancer cell line PANC-1, the cells were treated with 0.01–2 μg/ml PKCα inhibitor Gö6976 for 24h. In western blots, a significant decrease of Snail and a significant increase of claudin-1 and occludin were observed after treatment with Gö6976 in a dose-dependent manner, whereas no changes of claudin-4 and -7 were observed compared with the control (Figure 2A; Supplementary Figure 1, available at *Carcinogenesis* Online). In real-time PCR, a significant decrease of Snail mRNA and a significant increase of claudin-1 mRNA were induced by treatment with Gö6976, whereas no change of occludin mRNA was observed (Figure 2B). In immunocytochemistry, claudin-1 and occludin were strongly observed at the membranes after treatment with Gö6976 compared with the control (Supplementary Figure 2, available at *Carcinogenesis* Online).

PKCα inhibitor upregulates claudin-1, -4, -7 and occludin and increases TER values in hTERT-HPDEs

To investigate the effects of the PKCα inhibitor on tight junction proteins in normal pancreatic duct epithelial cells, hTERT-HPDEs were treated with 1 and 2 μg/ml Gö6976 for 24h. In western blots, claudin-1,-4,-7 and occludin were significantly increased by treatment with Gö6976 (Figure 2C; Supplementary Figure 1, available at *Carcinogenesis* Online). In real-time PCR, claudin-1,-4,-7 and occludin mRNAs were significantly increased by treatment with Gö6976 (Figure 2D). In immunocytochemistry, claudin-1 and occludin were detected at the membranes after treatment with Gö6976 (Supplementary Figure 2, available at *Carcinogenesis* Online). Furthermore, to investigate whether the PKCα inhibitor affected barrier function in normal pancreatic duct epithelial cells, hTERT-HPDEs were treated with 1 μg/ml Gö6976 for 24h and then TER was measured. TER values were significantly increased from 2h after treatment with Gö6976 (Figure 2E).

PKCα inhibitor induces activation of MAPK/ERK in both PANC-1 cells and hTERT-HPDEs

PKCα functions as a potent activator of c-Raf-1 and turns on the MAPK/ERK cascade (36). Thus, we investigated the effect of Gö6976 on MAPK/ERK activation in pancreatic cancer cells and normal pancreatic duct epithelial cells. Western blots revealed that Gö6976 induced phosphorylation of MAPK of both PANC-1 cells and hTERT-HPDEs in a dose-dependent manner (Figure 3A and B; Supplementary Figure 3, available at *Carcinogenesis* Online).

MAPK/ERK inhibitor prevents upregulation of claudin-1 and occludin by treatment with PKCα inhibitor in PANC-1 cells, but not in hTERT-HPDEs

To investigate whether MAPK/ERK activation affected changes of claudin-1, occludin and Snail induced by treatment with Gö6976, PANC-1 cells and hTERT-HPDEs were pretreated with 20 μM MAPK inhibitor U0126 before treatment with 1 μg/ml Gö6976. In western blots, U0126 prevented upregulation of phospho-MAPK (pMAPK) after treatment with Gö6976 in both PANC-1 cells and hTERT-HPDEs (Figure 3C and D; Supplementary Figure 3, available at *Carcinogenesis* Online). In PANC-1 cells, U0126 prevented upregulation of claudin-1 and occludin after treatment with Gö6976, whereas downregulation of Snail was decreased (Figure 3C; Supplementary Figure 3, available at *Carcinogenesis* Online). In hTERT-HPDEs, upregulation of occludin after treatment with Gö6976 was enhanced by treatment with U0126, whereas upregulation of claudin-1 was not affected by the treatment (Figure 3D; Supplementary Figure 3, available at *Carcinogenesis* Online).

Upregulation of claudin-1 by treatment with PKCα inhibitor is involved in distinct signaling pathways in PANC-1 cells and in hTERT-HPDEs

As shown in Figure 3, MAPK inhibitor U0126 prevented upregulation of claudin-1 after treatment with Gö6976 in PANC-1 cells but not in hTERT-HPDEs. To investigate which signaling pathways were associated with induction of claudin-1 by Gö6976 in PANC-1 cells and hTERT-HPDEs, the cells were pretreated with U0126, p38 MAPK inhibitor SB203580, PI3K inhibitor LY294002, panPKC inhibitor GF109203X, JNK inhibitor SP600125 and NF-κB inhibitor IMD-0354 before treatment with Gö6976. In western blots, induction of claudin-1 after treatment with Gö6976 was inhibited by U0126, SB203580, LY294002 and GF109203X in PANC-1 cells (Figure 3E; Supplementary Figure 3, available at *Carcinogenesis* Online), whereas in hTERT-HPDEs, induction of claudin-1 after treatment with Gö6976 was inhibited by SB203580, LY294002, GF109203X, SP600125 and IMD-0354 (Figure 3F; Supplementary Figure 3, available at *Carcinogenesis* Online).

TGF-β1 upregulates Snail and downregulates claudin-1, -4 and occludin together with activation of pPKCα and pMAPK/ERK in PANC-1 cells

To investigate changes of Snail and claudins/occludin caused by PKCα and MAPK/ERK during EMT induced by TGF-β in PANC-1 cells, the cells were treated with 100 ng/ml TGF-β1 for 24 and 48h. PANC-1 cells acquired a spindle cell morphology from 24h after treatment with TGF-β1 (Supplementary Figure 4, available at *Carcinogenesis* Online). In western blots, claudin-1,-4 and occludin were decreased and Snail was increased at 24 and 48h after treatment with TGF-β1, whereas no change of claudin-7 was observed (Figure 4A; Supplementary Figure 5, available at *Carcinogenesis* Online). Furthermore, TGF-β1 enhanced phosphorylation of PKCα and MAPK/ERK at 24 and 48h, respectively (Figure 4A; Supplementary Figure 5, available at *Carcinogenesis* Online).

TGF-β1 downregulates claudin-1, -7 and occludin and upregulates claudin-4 in hTERT-HPDEs

To investigate changes of claudins/occludin, Snail, PKCα and MAPK induced by treatment with TGF-β1 in hTERT-HPDEs, the cells were pretreated with 4% FBS for 24h and then treated with 20 ng/ml TGF-β1 for 24 and 48h. In phase-contrast images, hTERT-HPDEs also acquired spindle cell morphology from 24h after treatment with TGF-β1 (Supplementary Figure 4, available at *Carcinogenesis* Online). In western blots, claudin-1 and occludin were decreased and claudin-4

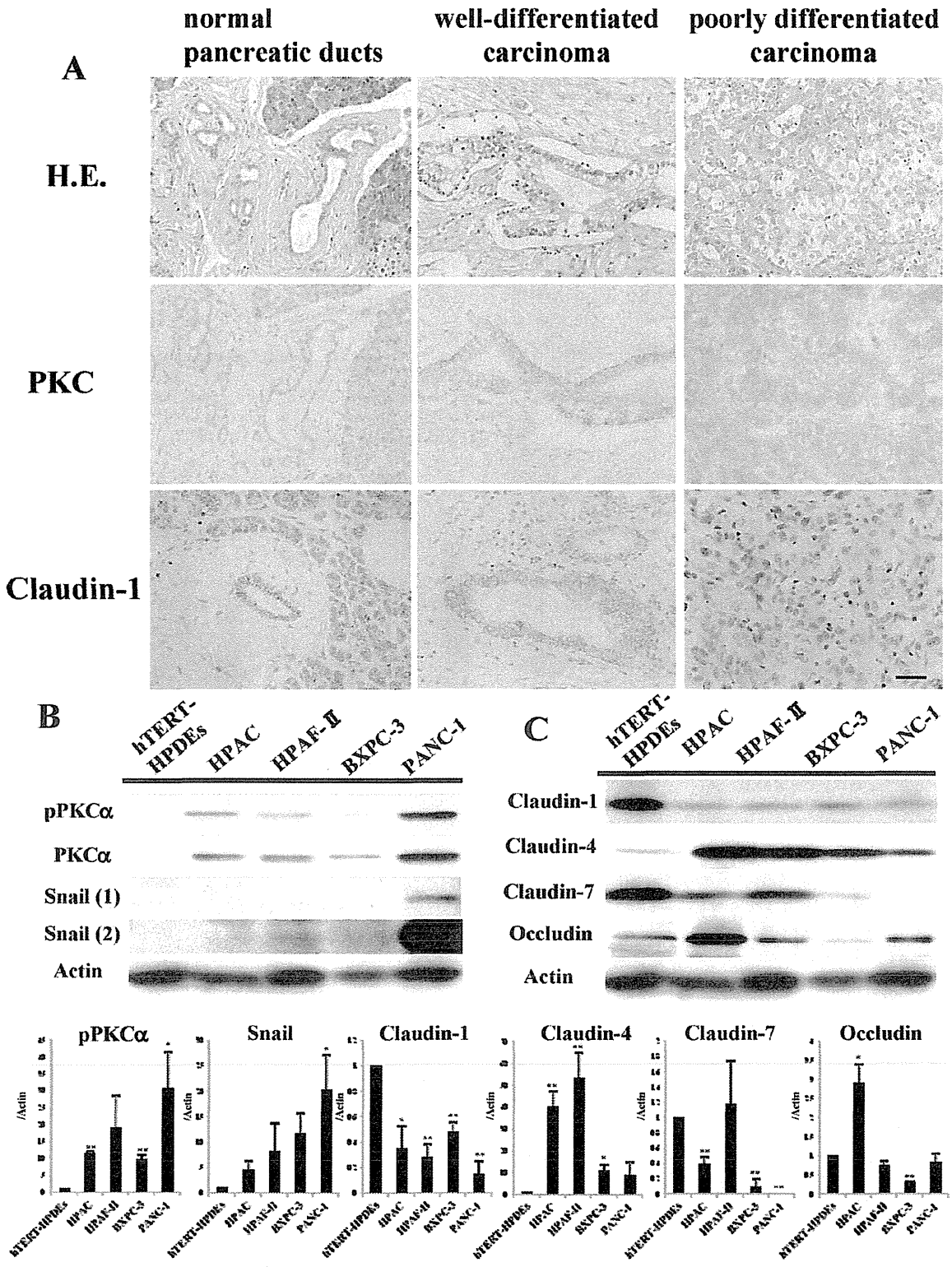

Fig. 1. (**A**) Hematoxylin and eosin staining and immunohistochemical staining for PKCα and claudin-1 in normal pancreatic ducts, well- and poorly differentiated pancreatic carcinomas. Bar: 50 μm. (**B** and **C**) Western blotting for pPKCα, panPKCα (PKCα), Snail, claudin-1, -4, -7 and occludin in normal pancreatic duct epithelial cells (hTERT-HPDEs) and pancreatic cancer cell lines HPAC, HPAF-II, BXPC-3 and PANC-1. Snail (1): exposed to X-ray film for 1 min. Snail (2): exposed to X-ray film for 20 min. The corresponding expression levels of B and C are shown as bar graphs. $n = 3$, $^{*}P < 0.05$ and $^{**}P < 0.01$ versus hTERT-HPDEs.

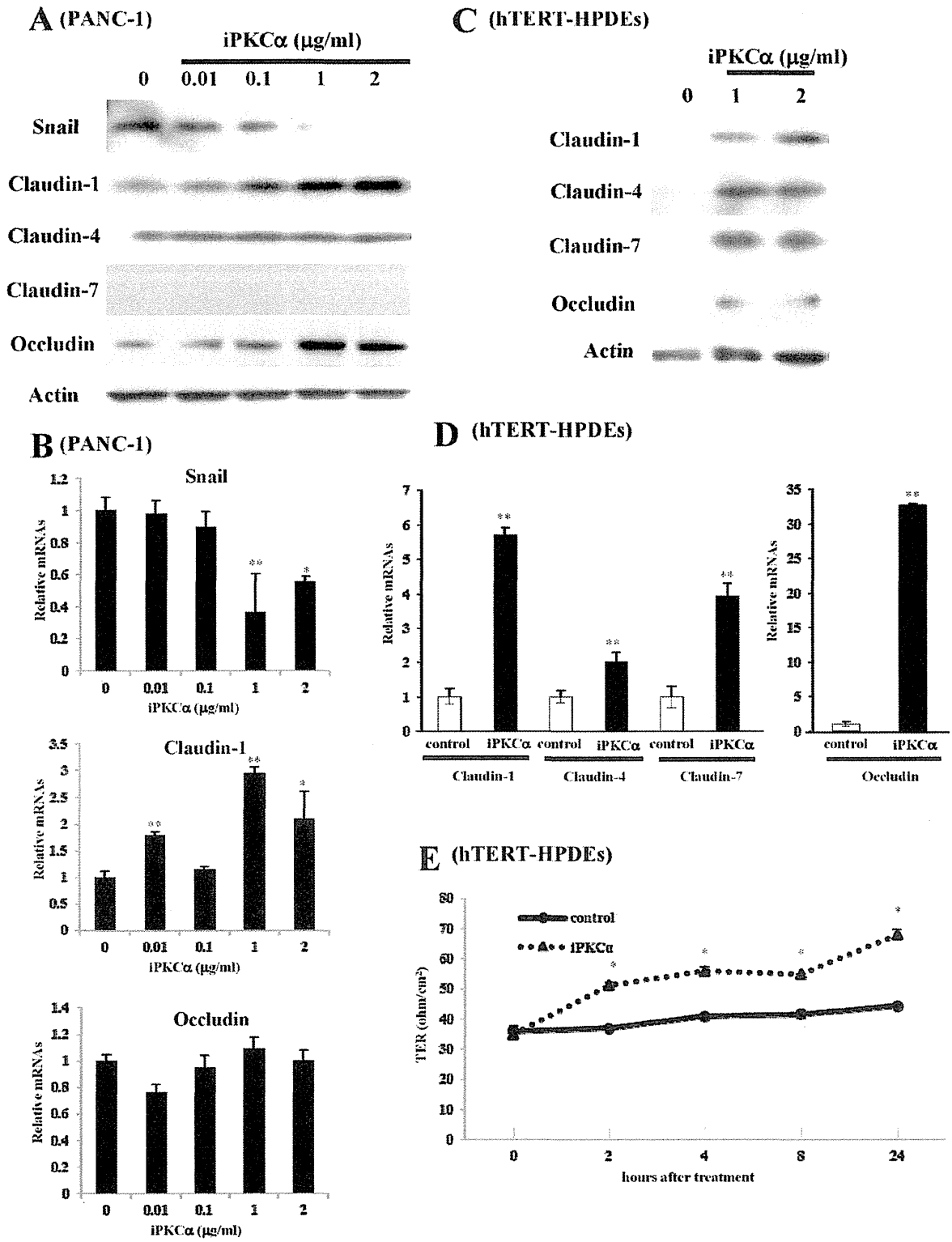

Fig. 2. (**A**) Western blotting for Snail, claudin-1, -4, -7 and occludin in PANC-1 cells after treatment with 0–2 μg/ml Gö6976 for 24 h. (**B**) Real-time PCR for Snail, claudin-1 and occludin in PANC-1 cells after treatment with 0–2 μg/ml Gö6976 for 24 h. (**C**) Western blotting for claudin-1, -4, -7 and occludin in hTERT-HPDEs after treatment with 1 and 2 μg/ml Gö6976 for 24 h. (**D**) Real-time PCR for claudin-1, -4, -7 and occludin in hTERT-HPDEs after treatment with 1 μg/ml Gö6976 for 24 h. (**E**) TER values in hTERT-HPDEs after treatment with 1 μg/ml Gö6976 for 24 h. iPKCα: PKCα inhibitor Gö6976. $n = 3$. $^{*}P < 0.05$ and $^{**}P < 0.01$ versus control (0 μg/ml).

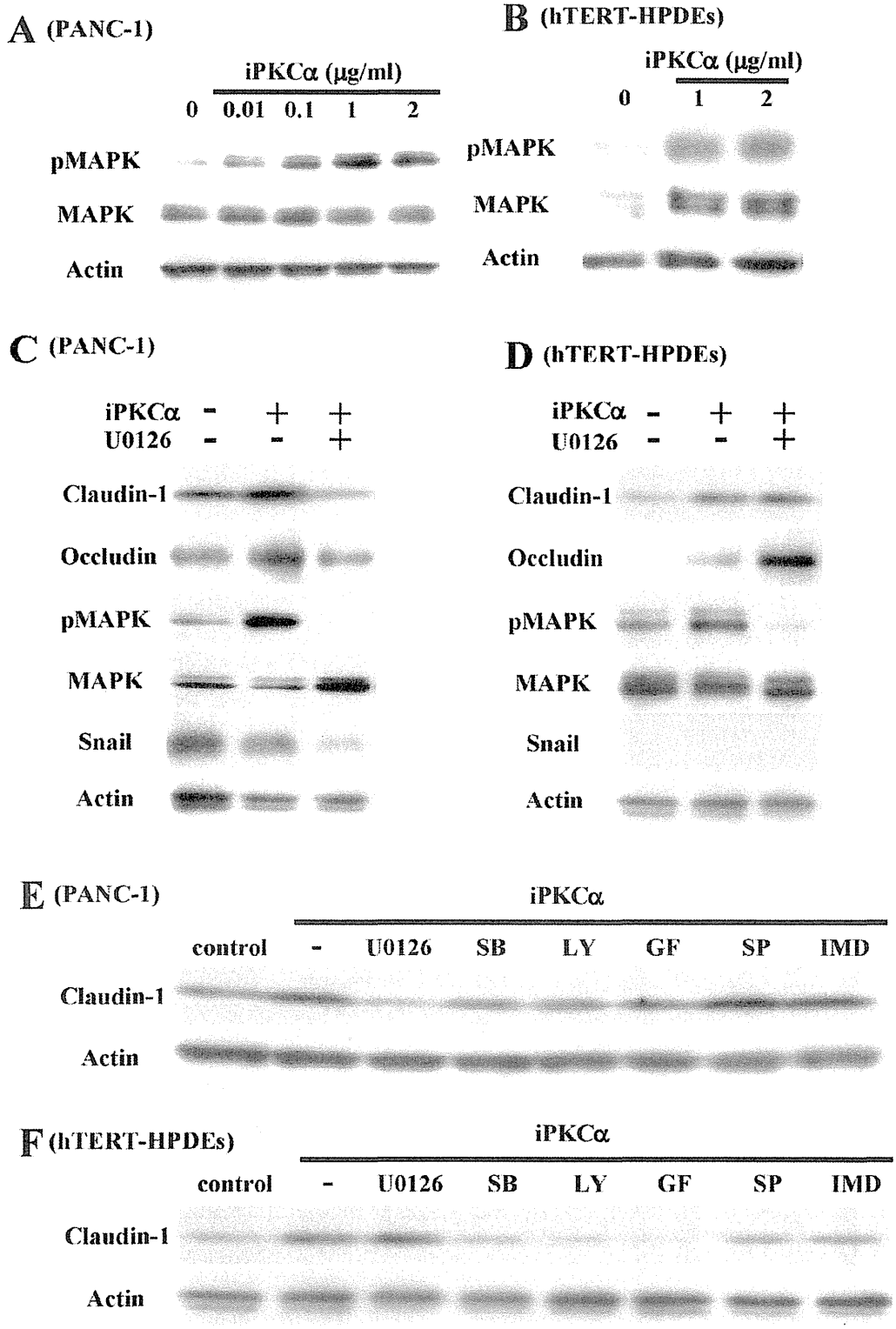

Fig. 3. Western blotting for pMAPK and panMAPK (MAPK) in PANC-1 cells (**A**) and hTERT-HPDEs (**B**) after treatment with 0–2 μg/ml Gö6976 for 24h. Western blotting for claudin-1, occludin, pMAPK, MAPK and Snail in PANC-1 cells (**C**) and hTERT-HPDEs (**D**) pretreated with 20 μM MAPK/ERK inhibitor U0126 before treatment with 1 μg/ml Gö6976 for 24h. Western blotting for claudin-1 in PANC-1 cells (**E**) and hTERT-HPDEs (**F**) pretreated with 20 μM MAPK/ERK inhibitor U0126, 10 μM p38 MAPK inhibitor SB203580 (SB), 10 μM PI3K inhibitor LY294002 (LY), 10 μM panPKC inhibitor GF109203X (GF), 10 μM JNK inhibitor SP600125 (SP) and 0.1 μM NF-κB inhibitor IMD-0354 (IMD) before treatment with 1 μg/ml PKCα inhibitor Gö6976 for 24h. iPKCα: PKCα inhibitor Gö6976.

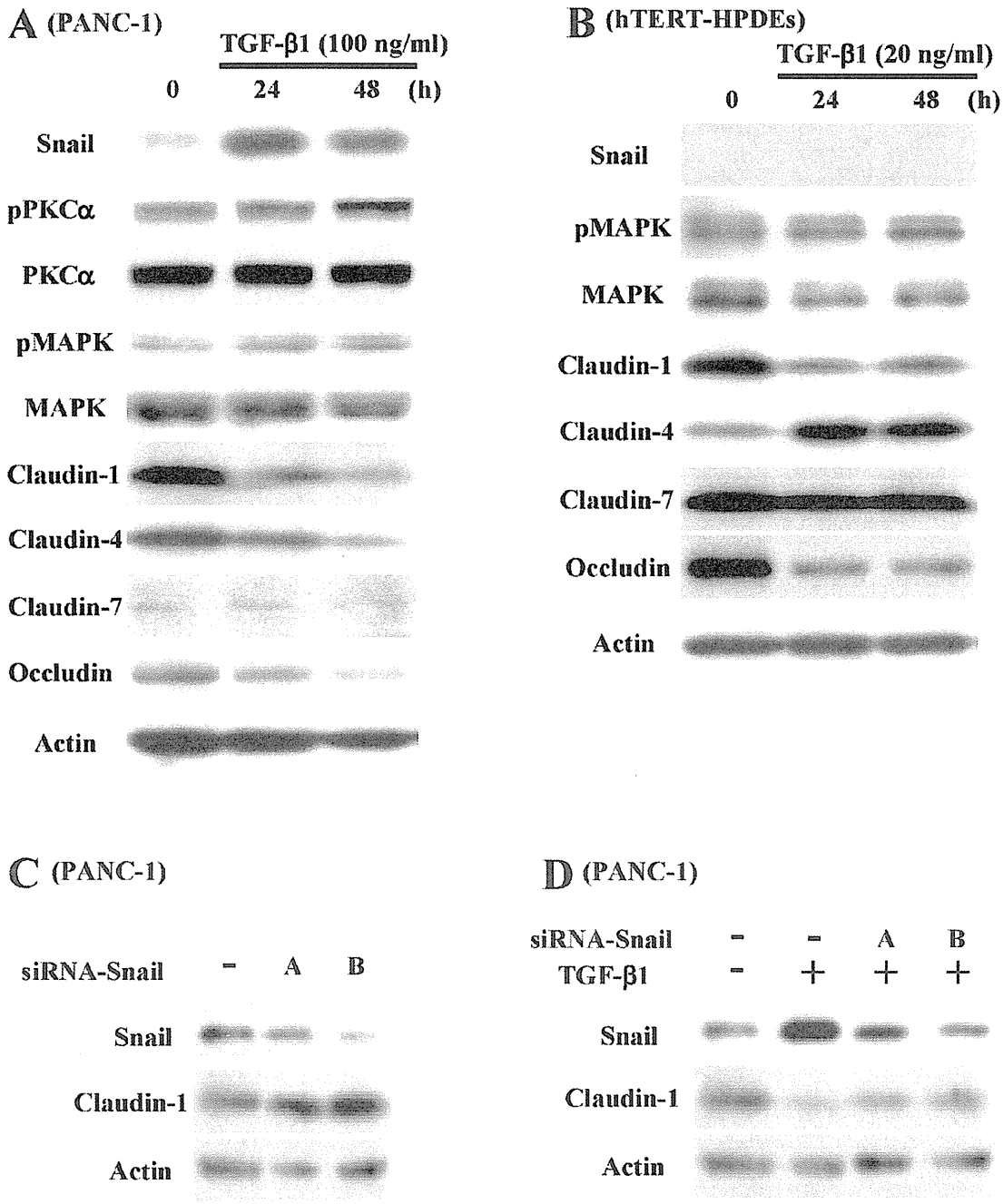

Fig. 4. (**A**) Western blotting for Snail, pPKCα, panPKCα (PKCα), pMAPK, panMAPK (MAPK), claudin-1, -4, -7 and occludin in PANC-1 cells after treatment with 100 ng/ml TGF-β1 for 24 and 48 h. (**B**) Western blotting for claudin-1, -4, -7, occludin, Snail, PKCα, pMAPK and MAPK in hTERT-HPDEs after treatment with 20 ng/ml TGF-β1 for 24 and 48 h. (**C**) Western blotting for Snail and claudin-1 in PANC-1 cells treated with siRNAs of Snail. (**D**) Western blotting for Snail and claudin-1 in PANC-1 cells treated with siRNAs of Snail and 100 ng/ml TGF-β1 for 48 h. Control cells in Figure 4C and D are transfected with a scrambled siRNA. KD: knockdown.

was increased at 24 and 48 h after treatment with TGF-β1, whereas no changes of claudin-7 and pMAPK/ERK were observed and Snail and PKCα were not detected (Figure 4B; Supplementary Figure 5, available at *Carcinogenesis* Online).

Claudin-1 in PANC-1 cells is in part regulated via the Snail gene

To investigate whether claudin-1 in PANC-1 cells was directly regulated *via* the Snail gene, knockdown of Snail using siRNAs was performed and the cells were treated with or without 100 ng/ml TGF-β1 for 48 h. In the control cells, claudin-1 was significantly increased by knockdown of Snail (Figure 4C; Supplementary Figure 5, available at *Carcinogenesis* Online). In the cells treated with TGF-β1, regardless of the fact that an increase of TGF-β1-induced Snail was prevented by the siRNAs, the downregulation of claudin-1 by TGF-β1 was not completely reversed (Figure 4D). These findings indicated that claudin-1 in PANC-1 cells during

EMT induced by TGF-β, was in part regulated *via* the Snail gene, though also by other factors.

PKCα inhibitor prevents upregulation of Snail and downregulation of claudin-1 by TGF-β in PANC-1 cells

To investigate whether the PKCα inhibitor affected changes of Snail, claudins/occludin and pMAPK/ERK induced by TGF-β in PANC-1 cells, the cells were pretreated with Gö6976 before treatment with 100ng/ml TGF-β1. Western blots showed that Gö6976 prevented the increase of Snail and decrease of claudin-1 after treatment with TGF-β1, but it did not affect the changes of claudin-4, -7 and occludin (Figure 5A; Supplementary Figure 6, available at *Carcinogenesis* Online). Gö6976 enhanced the upregulation of pMAPK/ERK caused by treatment with TGF-β1 (Figure 5A; Supplementary Figure 6, available at *Carcinogenesis* Online).

PKCα inhibitor prevents downregulation of claudin-1 and occludin and enhanced upregulation of claudin-4 by TGF-β in hTERT-HPDEs

hTERT-HPDEs were pretreated with 4% FBS for 24h and then treated with Gö6976 before treatment with 20ng/ml TGF-β1. Gö6976 prevented decreases of claudin-1 and occludin after treatment with TGF-β1 and enhanced the increase of claudin-4, whereas it did not affect claudin-7 or pMAPK/ERK (Figure 5B; Supplementary Figure 6, available at *Carcinogenesis* Online). After treatment with TGF-β1, PKCα was not detected with or without Gö6976 (Figure 5B; Supplementary Figure 6, available at *Carcinogenesis* Online).

PKCα inhibitor prevents upregulation of Snail and pPKCα and downregulation of claudin-1 and pMAPK/ERK under hypoxia in PANC-1 cells

To investigate whether the PKCα inhibitor affected changes of Snail, claudin-1, occludin, pPKCα and pMAPK/ERK caused by hypoxia in PANC-1 cells, the cells were incubated in a 2% CO_2:2% O_2 incubator balanced with nitrogen for 24h with or without Gö6976. In western blots, in PANC-1 cells under hypoxia, increases of Snail and pPKCα and decreases of claudin-1 and pMAPK/ERK were observed compared with the control (Figure 5C; Supplementary Figure 6, available at *Carcinogenesis* Online). Gö6976 prevented these increases of Snail and pPKCα and decreases of claudin-1 and pMAPK, whereas no change of occludin was observed under hypoxia with or without Gö6976 (Figure 5C; Supplementary Figure 6, available at *Carcinogenesis* Online).

PKCα inhibitor enhances upregulation of claudin-1, -4, -7 and occludin under hypoxia in hTERT-HPDEs

To investigate whether the PKCα inhibitor affected changes of Snail, claudin-1, -4, -7, occludin and pMAPK/ERK in hTERT-HPDEs caused by hypoxia, the cells were pretreated with 4% FBS for 24h and were incubated in a 2% CO_2:2% O_2 incubator balanced with nitrogen for 24h with or without Gö6976. In western blots, increases of claudin-1, -4, -7, occludin and pMAPK/ERK caused by hypoxia were observed (Figure 5D; Supplementary Figure 6, available at *Carcinogenesis* Online). Gö6976 enhanced increases of claudin-1, -4, -7 and occludin under hypoxia, whereas it did not affect upregulation of pMAPK/ERK (Figure 5D; Supplementary Figure 6, available at *Carcinogenesis* Online). Snail was not detected under hypoxia with or without Gö6976 (Figure 5D; Supplementary Figure 6, available at *Carcinogenesis* Online).

PKCα inhibitor prevents downregulation of barrier function and fence function by treatment with TGF-β1 in HPAC cells

To investigate whether the PKCα inhibitor affected the barrier and fence functions in pancreatic cancer cells, the well-differentiated pancreatic cancer cell line HPAC was used. It was pretreated with 100ng/ml TGF-β1 for 24 and 48h with or without Gö6976. In western blots, upregulation of Snail and pPKCα and downregulation of claudin-1,-4, -7 and occludin were observed after treatment with TGF-β1 together with downregulation of the barrier and fence functions (Figure 6A, C and D; Supplementary Figure 7, available at *Carcinogenesis* Online). Gö6976 prevented upregulation of Snail and downregulation of claudin-1 after treatment with TGF-β1, whereas it did not affect changes of claudin-4, -7 and occludin (Figure 6B; Supplementary Figure 7, available at *Carcinogenesis* Online). These changes were similar to the changes in PANC-1 cells. Furthermore, Gö6976 prevented downregulation of the barrier and fence functions by TGF-β1 (Figure 6C and D).

Discussion

In this study, we demonstrated that PKCα inhibitor Gö6976 protected against downregulation of claudin-1 *via* Snail- and MAPK/ERK-dependent pathways during EMT in human pancreatic cancer. The mechanisms involved in the regulation of claudin-1 by the inhibitor in pancreatic cancer were in part different from those in normal HPDEs.

It is known that the PKC inhibitor Gö6976, which was used in this study, can inhibit not only α isoform of PKC but also β1 isoform of PKC. To clarify a role of PKCα in the regulation of claudins during EMT in pancreatic cancer, we performed using siRNA against PKCα or PKCβ. In PANC-1 cells, knockdown of PKCα by the siRNA induced claudin-1 and -4 and prevented downregulation of claudin-1 and -4 by treatment with TGF-β1, whereas the effects of knockdown of PKCβ by the siRNA were not observed (Supplementary Figure 8, available at *Carcinogenesis* Online). These results indicated that in this study, the effects of the PKC inhibitor Gö6976 were mainly caused *via* a specific PKCα pathway.

PKCα is thought to be one of the biomarkers for diagnosis of cancer and regulators in cancer cells (7,10). In pancreatic cancer, cell proliferation and tumorigenicity are directly related to PKCα expression (8,9). On the other hand, PKC is associated with claudin-1 expression in melanoma cells (37). In HPAC cells, treatment with TPA modifies the activity of pPKCα and causes downregulation of claudin-1 and mislocalization of claudin-4 and occludin (13). In this study, in poorly differentiated human pancreatic cancer tissues and the pancreatic cancer cell line PANC-1, overexpression of PKCα and downregulation of claudin-1 were observed, whereas in normal HPDEs *in vivo* and *in vitro*, PKCα was not detected and claudin-1 was highly expressed. These findings suggest that, in pancreatic cancer, PKCα is a biomarker for diagnosis and may be a negative regulator against claudin-1 expression.

The activation of PKC is involved in EMT. The PKC activator TPA induces EMT in human prostate cancer cells and HPAC cells (12,13). Expression of PKCα and PKCδ closely contributes to EMT in colon cancer cells (14,15). TGF-β1 induces PKCα in poorly differentiated pancreatic cancer cell line BXPC-3 (38). During EMT induced by treatment with TGF-β1 and under hypoxia, claudin-1 is directly regulated *via* the Snail gene (28). In this study, treatment with the PKCα inhibitor Gö6976 transcriptionally decreased Snail and increased claudin-1 in PANC-1 cells. Expression of claudin-1 in PANC-1 cells was increased by knockdown of Snail. Furthermore, the PKCα inhibitor prevented the upregulation of Snail and downregulation of claudin-1 in PANC-1 cells during EMT induced by treatment with TGF-β1 and hypoxia. These findings suggested that, in pancreatic cancer cells, PKCα is activated by TGF-β1 and hypoxia induced EMT, and the PKCα inhibitor could prevent downregulation of claudin-1 by repressing Snail during EMT.

PKC has been shown to induce both assembly and disassembly of tight junctions depending on the cell type and conditions of activation (39–41). It is also known to regulate epithelial barrier function *via* tight junctions (42,43). We previously reported that, in hTERT-HPDEs, TPA enhanced expression of claudin-1, -4, -7 and -18, occludin, JAM-A, ZO-1, ZO-2 and tricellulin, and the expression of claudin-4 and -18 induced by TPA was inhibited by the PKCα inhibitor Gö6976 (32,34). In this study, using hTERT-HPDEs, treatment with the PKCα inhibitor transcriptionally induced expression of claudin-1, -4, -7 and occludin and enhanced the barrier function measured as the TER value. Furthermore, in hTERT-HPDEs, TGF-β1

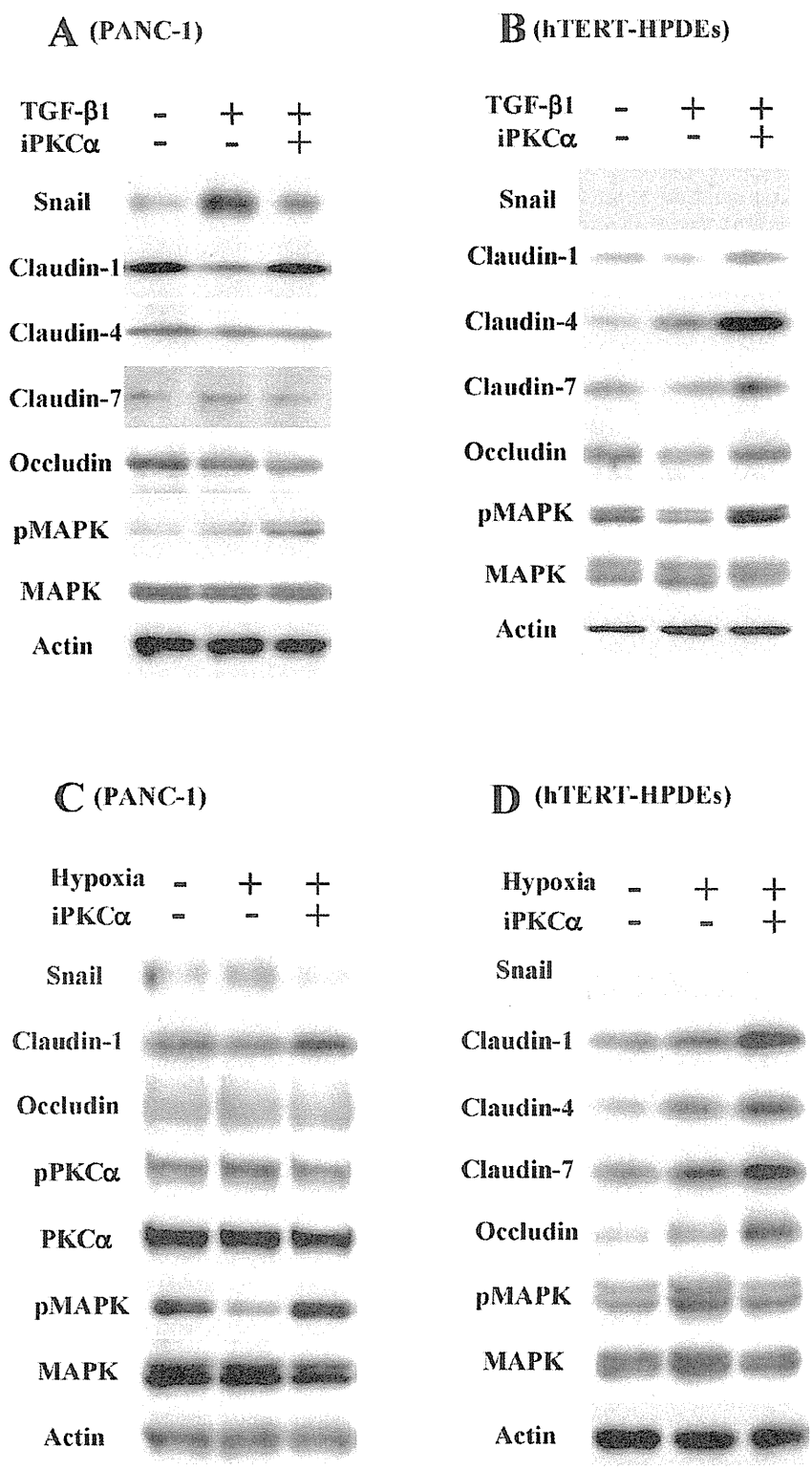

Fig. 5. (**A**) Western blotting for Snail, claudin-1, -4, -7, occludin, pMAPK and panMAPK (MAPK) in PANC-1 cells pretreated with 1 μg/ml Gö6976 before treatment with 100 ng/ml TGF-β1 for 24 h. (**B**) Western blotting for claudin-1, -4, -7, occludin, Snail, panPKCα (PKCα), pMAPK and MAPK in hTERT-HPDEs pretreated with 1 μg/ml Gö6976 before treatment with 20 ng/ml TGF-β1 for 24 h. (**C**) Western blotting for Snail, claudin-1, occludin, pPKCα, PKCα, pMAPK and MAPK in PANC-1 cells with or without 1 μg/ml Gö6976 under hypoxia for 24 h. (**D**) Western blotting for claudin-1, -4, -7, occludin, pMAPK, MAPK and Snail in hTERT-HPDEs with or without 1 μg/ml Gö6976 under hypoxia for 24 h. iPKCα: PKCα inhibitor Gö6976.

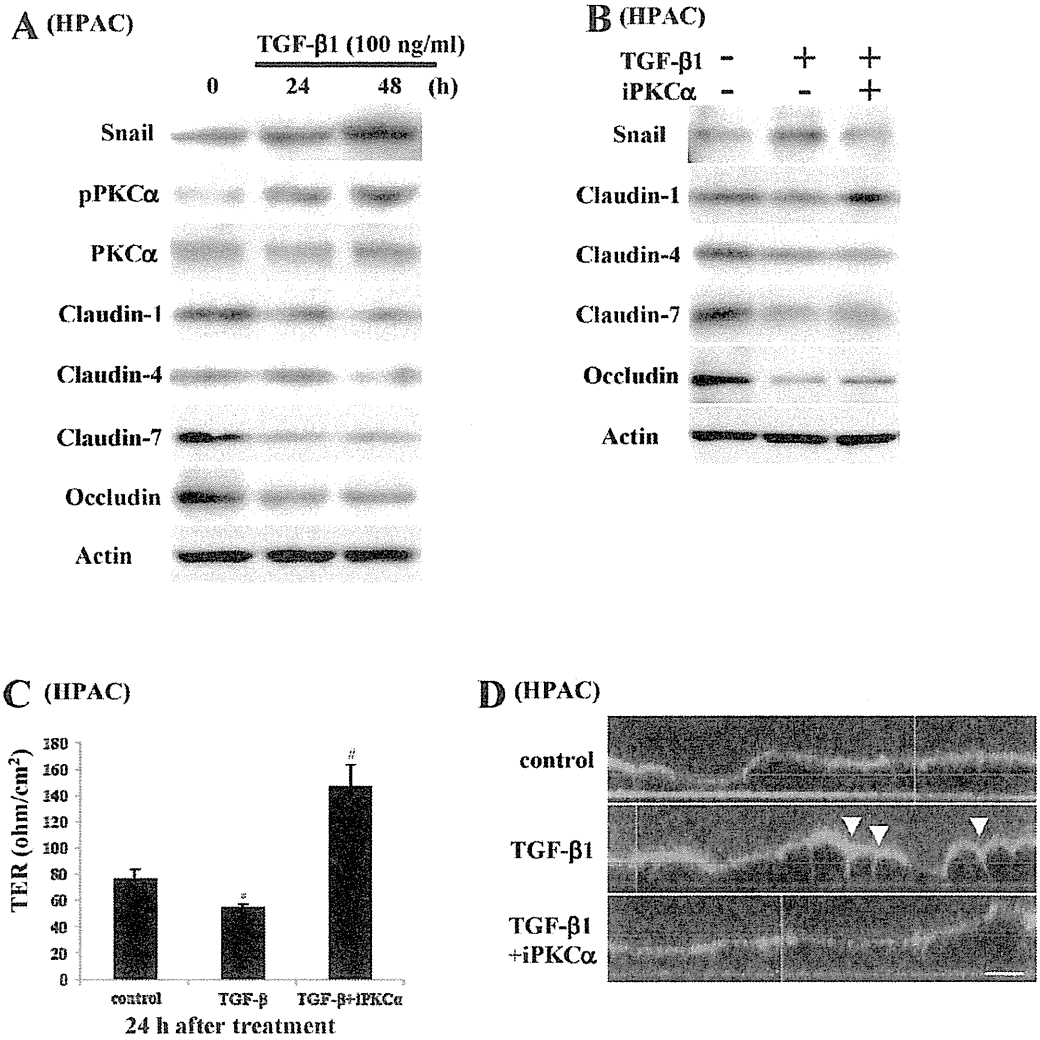

Fig. 6. (**A**) Western blotting for Snail, pPKCα, panPKCα (PKCα), claudin-1, -4, -7 and occludin in HPAC cells after treatment with 100 μg/ml TGF-β1 for 24 and 48 h. (**B**) Western blotting for Snail, pPKCα, PKCα, claudin-1, -4, -7 and occludin in HPAC cells pretreated with 1 μg/ml Gö6976 before treatment with 100 ng/ml TGF-β1 for 24 h. (**C**) TER values in HPAC cells pretreated with 100 ng/ml TGF-β1 for 24 h with or without 1 μg/ml Gö6976. (**D**) Fence function examined by diffusion of labeled BODIPY-sphingomyelin into HPAC cells pretreated with 100 ng/ml TGF-β1 for 24 h with or without 1 μg/ml Gö6976. In HPAC cells treated with TGF-β1, the probe strongly labels the basolateral surface and appears to penetrate the cells (arrowheads), whereas the probe is effectively retained in the apical domain of the control cells and the cells were treated with TGF-β1 and Gö6976. Bar: 20 μm. iPKCα: PKCα inhibitor Gö6976.

caused downregulation of claudin-1 and occludin and upregulation of claudin-4. The PKCα inhibitor prevented the downregulation of claudin-1 and occludin and enhanced the upregulation of claudin-4. However, expression of Snail in hTERT-HPDE treated with the PKCα inhibitor and TGF-β1 was not detected. We have previously reported that treatment with TGF-β1 upregulates claudin-4 without a change of barrier function in normal human nasal epithelial cells (43). TGF-β1 transcriptionally upregulates claudin-4 and strengthens the intestinal barrier in a human intestinal cell line (44). TGF-β1 induces EMT in cultured human pancreatic duct cells (45). Our results indicated that the PKCα inhibitor upregulated tight junction proteins and the barrier function *via* a Snail-independent pathway in normal HPDEs. Furthermore, the PKCα inhibitor also prevented downregulation of claudin-1 *via* a Snail-independent pathway during EMT induced by treatment with TGF-β in normal HPDEs.

Activated PKCα turns on the MAPK cascade *via* activation of downstream signaling (46). PKCα inhibition leads to increased ERK1/2 activity (47,48). The arrangement of the expression and distribution of claudin-1 are closely related to cell dissociation status in pancreatic cancer cells through the MAPK/ERK pathway (49). In this study, the PKCα inhibitor Gö6976 enhanced the phosphorylation of MAPK/ERK in both PANC-1 cells and hTERT-HPDEs. In PANC-1 cells, the upregulation of claudin-1, but not the downregulation of Snail, by the PKCα inhibitor was prevented by the MAPK/ERK inhibitor U0126. In PANC-1 cells treated with TGF-β1, the downregulation of claudin-1 by TGF-β1 was not completely reversed *via* knockdown of Snail. In hTERT-HPDEs, the upregulation of claudin-1 by the PKCα inhibitor was prevented by treatment with inhibitors of p38MAPK, PI3K, panPKC, JNK and NF-κB, but not MAPK/ERK signaling pathways. These findings suggested that the signal transduction pathways of the PKCα inhibitor for the regulation of claudin-1 were different in pancreatic cancer cells and normal HPDEs, and in pancreatic cancer, claudin-1 was regulated *via* not only the Snail gene but also the MAPK/ERK signaling pathway.

Loss of the fence function, which is important for maintenance of epithelial cell polarity, is closely associated with the expression of

claudin-1 (24). The poorly differentiated pancreatic cancer cell line PANC-1 shows loss of the tight junctional barrier measured as TER and the fence function examined by diffusion of labeled BODIPY-sphingomyelin (28). The well-differentiated pancreatic cancer cell line HPAC has high barrier and fence functions, and the fence function is downregulated by treatment with TGF-β1 and hypoxia (28). In this study, upregulation of Snail and downregulation of claudin-1 expression, barrier function and fence function were observed in HPAC cells treated with TGF-β1, and the PKCα inhibitor Gö6976 prevented all the changes induced by treatment with TGF-β1. These results suggest that the PKCα inhibitor may prevent downregulation of epithelial cell polarity during EMT in pancreatic cancer.

In conclusion, the PKCα inhibitor strongly protected against downregulation of claudin-1 during EMT in pancreatic cancer. Furthermore, in normal HPDEs, the PKCα inhibitor induced some tight junction proteins, including claudin-1, and enhanced barrier function. Taken together, these results suggest that PKCα inhibitors may be potential therapeutic agents against the malignancy of human pancreatic cancer cells.

Supplementary material

Supplementary Figures 1–8 can be found at http://carcin.oxfordjournals.org/

Funding

Memorial Foundation; the Pancreas Research Foundation of Japan and Program for developing the supporting system for upgrading education and research; the Ministry of Education, Culture, Sports Science and Technology and the Ministry of Health, Labour and Welfare of Japan.

Conflict of Interest Statement: None declared.

References

1. Siegel,R. *et al.* (2011) Cancer statistics, 2011: the impact of eliminating socioeconomic and racial disparities on premature cancer deaths. *CA. Cancer J. Clin.*, **61**, 212–236.
2. Mackay,H.J. *et al.* (2007) Targeting the protein kinase C family: are we there yet? *Nat. Rev. Cancer*, **7**, 554–562.
3. Ali,A.S. *et al.* (2009) Exploitation of protein kinase C: a useful target for cancer therapy. *Cancer Treat. Rev.*, **35**, 1–8.
4. Newton,A.C. (1997) Regulation of protein kinase C. *Curr. Opin. Cell Biol.*, **9**, 161–167.
5. El-Rayes,B.F. *et al.* (2008) Protein kinase C: a target for therapy in pancreatic cancer. *Pancreas*, **36**, 346–352.
6. Scotti,M.L. *et al.* (2010) Protein kinase Ciota is required for pancreatic cancer cell transformed growth and tumorigenesis. *Cancer Res.*, **70**, 2064–2074.
7. Kang,J.H. *et al.* (2009) Plasma protein kinase C (PKC)alpha as a biomarker for the diagnosis of cancers. *Carcinogenesis*, **30**, 1927–1931.
8. Denham,D.W. *et al.* (1998) Directed antisense therapy confirms the role of protein kinase C-alpha in the tumorigenicity of pancreatic cancer. *Surgery*, **124**, 218–23.
9. Zhang,X. *et al.* (1997) Inhibition of expression of PKC-alpha by antisense mRNA is associated with diminished cell growth and inhibition of amylase secretion by AR4-2J cells. *Exp. Cell Res.*, **233**, 225–231.
10. Konopatskaya,O. *et al.* (2010) Protein kinase Calpha: disease regulator and therapeutic target. *Trends Pharmacol. Sci.*, **31**, 8–14.
11. Thiery,J.P. *et al.* (2009) Epithelial-mesenchymal transitions in development and disease. *Cell*, **139**, 871–890.
12. He,H. *et al.* (2010) Phorbol ester phorbol-12-myristate-13-acetate induces epithelial to mesenchymal transition in human prostate cancer ARCaPE cells. *Prostate*, **70**, 1119–1126.
13. Kyuno,D. *et al.* (2011) Protein kinase Cα inhibitor enhances the sensitivity of human pancreatic cancer HPAC cells to *Clostridium perfringens* enterotoxin via claudin-4. *Cell Tissue Res.*, **346**, 369–381.
14. Ghoul,A. *et al.* (2009) Epithelial-to-mesenchymal transition and resistance to ingenol 3-angelate, a novel protein kinase C modulator, in colon cancer cells. *Cancer Res.*, **69**, 4260–4269.
15. Masur,K. *et al.* (2001) High PKC alpha and low E-cadherin expression contribute to high migratory activity of colon carcinoma cells. *Mol. Biol. Cell*, **12**, 1973–1982.
16. Ikenouchi,J. *et al.* (2003) Regulation of tight junctions during the epithelium-mesenchyme transition: direct repression of the gene expression of claudins/occludin by Snail. *J. Cell. Sci.*, **116**(Pt 10), 1959–1967.
17. Karanjawala,Z.E. *et al.* (2008) New markers of pancreatic cancer identified through differential gene expression analyses: claudin 18 and annexin A8. *Am. J. Surg. Pathol.*, **32**, 188–196.
18. Michl,P. *et al.* (2003) Claudin-4 expression decreases invasiveness and metastatic potential of pancreatic cancer. *Cancer Res.*, **63**, 6265–6271.
19. Cereijido,M. *et al.* (1998) Role of tight junctions in establishing and maintaining cell polarity. *Annu. Rev. Physiol.*, **60**, 161–177.
20. Gumbiner,B.M. (1993) Breaking through the tight junction barrier. *J. Cell Biol.*, **123**(6 Pt 2), 1631–1633.
21. Schneeberger,E.E. *et al.* (1992) Structure, function, and regulation of cellular tight junctions. *Am. J. Physiol.*, **262**(6 Pt 1), L647–L661.
22. van Meer,G. *et al.* (1986) The tight junction does not allow lipid molecules to diffuse from one epithelial cell to the next. *Nature*, **322**, 639–641.
23. Martin,T.A. *et al.* (2009) Loss of tight junction barrier function and its role in cancer metastasis. *Biochim. Biophys. Acta*, **1788**, 872–891.
24. Kojima,T. *et al.* (2008) Transforming growth factor-beta induces epithelial to mesenchymal transition by down-regulation of claudin-1 expression and the fence function in adult rat hepatocytes. *Liver Int.*, **28**, 534–545.
25. Oku,N. *et al.* (2006) Tight junction protein claudin-1 enhances the invasive activity of oral squamous cell carcinoma cells by promoting cleavage of laminin-5 gamma2 chain via matrix metalloproteinase (MMP)-2 and membrane-type MMP-1. *Cancer Res.*, **66**, 5251–5257.
26. Singh,A.B. *et al.* (2011) Claudin-1 up-regulates the repressor ZEB-1 to inhibit E-cadherin expression in colon cancer cells. *Gastroenterology*, **141**, 2140–2153.
27. Yoon,C.H. *et al.* (2010) Claudin-1 acts through c-Abl-protein kinase Cdelta (PKCdelta) signaling and has a causal role in the acquisition of invasive capacity in human liver cells. *J. Biol. Chem.*, **285**, 226–233.
28. Kojima,T. *et al.* (2011) Downregulation of tight junction-associated MARVEL protein marvelD3 during epithelial-mesenchymal transition in human pancreatic cancer cells. *Exp. Cell Res.*, **317**, 2288–2298.
29. González-Mariscal,L. *et al.* (2008) Crosstalk of tight junction components with signaling pathways. *Biochim. Biophys. Acta*, **1778**, 729–756.
30. Kojima,T. *et al.* (2009) Tight junction proteins and signal transduction pathways in hepatocytes. *Histol. Histopathol.*, **24**, 1463–1472.
31. Kojima,T. *et al.* (2010) c-Jun N-terminal kinase is largely involved in the regulation of tricellular tight junctions via tricellulin in human pancreatic duct epithelial cells. *J. Cell. Physiol.*, **225**, 720–733.
32. Ito,T. *et al.* (2011) Transcriptional regulation of claudin-18 via specific protein kinase C signaling pathways and modification of DNA methylation in human pancreatic cancer cells. *J. Cell. Biochem.*, **112**, 1761–1772.
33. Kojima,T. *et al.* (2012) Regulation of tight junctions in human normal pancreatic duct epithelial cells and cancer cells. *Ann. N. Y. Acad. Sci.*, **1257**, 85–92.
34. Yamaguchi,H. *et al.* (2010) Transcriptional control of tight junction proteins via a protein kinase C signal pathway in human telomerase reverse transcriptase-transfected human pancreatic duct epithelial cells. *Am. J. Pathol.*, **177**, 698–712.
35. Deer,E.L. *et al.* (2010) Phenotype and genotype of pancreatic cancer cell lines. *Pancreas*, **39**, 425–435.
36. Kolch,W. *et al.* (1993) Protein kinase C alpha activates RAF-1 by direct phosphorylation. *Nature*, **364**, 249–252.
37. Leotlela,P.D. *et al.* (2007) Claudin-1 overexpression in melanoma is regulated by PKC and contributes to melanoma cell motility. *Oncogene*, **26**, 3846–3856.
38. Chen,Y. *et al.* (2010) PKCalpha-induced drug resistance in pancreatic cancer cells is associated with transforming growth factor-beta1. *J. Exp. Clin. Cancer Res.*, **29**, 104.
39. Andreeva,A.Y. *et al.* (2006) Assembly of tight junction is regulated by the antagonism of conventional and novel protein kinase C isoforms. *Int. J. Biochem. Cell Biol.*, **38**, 222–233.
40. Ellis,B. *et al.* (1992) Cellular variability in the development of tight junctions after activation of protein kinase C. *Am. J. Physiol.*, **263**(2 Pt 2), F293–F300.
41. Sjö,A. *et al.* (2003) Distinct effects of protein kinase C on the barrier function at different developmental stages. *Biosci. Rep.*, **23**, 87–102.
42. Balda,M.S. *et al.* (1993) Assembly of the tight junction: the role of diacylglycerol. *J. Cell Biol.*, **123**, 293–302.
43. Kurose,M. *et al.* (2007) Induction of claudins in passaged hTERT-transfected human nasal epithelial cells with an extended life span. *Cell Tissue Res.*, **330**, 63–74.

44. Hering,N.A. *et al.* (2011) Transforming growth factor-β, a whey protein component, strengthens the intestinal barrier by upregulating claudin-4 in HT-29/B6 cells. *J. Nutr.*, **141**, 783–789.
45. Shin,J.A. *et al.* (2011) Transforming growth factor-β induces epithelial to mesenchymal transition and suppresses the proliferation and transdifferentiation of cultured human pancreatic duct cells. *J. Cell. Biochem.*, **112**, 179–188.
46. Nakashima,S. (2002) Protein kinase C alpha (PKC alpha): regulation and biological function. *J. Biochem.*, **132**, 669–675.
47. Blobe,G.C. *et al.* (1993) Selective regulation of expression of protein kinase C (PKC) isoenzymes in multidrug-resistant MCF-7 cells. Functional significance of enhanced expression of PKC alpha. *J. Biol. Chem.*, **268**, 658–664.
48. Praskova,M. *et al.* (2002) Dual role of protein kinase C on mitogen-activated protein kinase activation and human keratinocyte proliferation. *Exp. Dermatol.*, **11**, 344–348.
49. Tan,X. *et al.* (2004) Arrangement of expression and distribution of tight junction protein claudin-1 in cell dissociation of pancreatic cancer cells. *Int. J. Oncol.*, **25**, 1567–1574.

Received October 29, 2012; revised January 13, 2013; accepted February 3, 2013

ANTICANCER RESEARCH *33*: 167-174 (2013)

Expression and Function of *FERMT* Genes in Colon Carcinoma Cells

KENJI KIRIYAMA[1,2,3], YOSHIHIKO HIROHASHI[1], TOSHIHIKO TORIGOE[1], TERUFUMI KUBO[1], YASUAKI TAMURA[1], TAKAYUKI KANASEKI[1], AKARI TAKAHASHI[1], EMIRI NAKAZAWA[1], ERI SAKA[1], CHARLOTTE RAGNARSSON[1], MUNEHIDE NAKATSUGAWA[1], SATOKO INODA[1,2], HIROKO ASANUMA[4], HIDEO TAKASU[5], TADASHI HASEGAWA[4], TAKAHIRO YASOSHIMA[3], KOICHI HIRATA[2] and NORIYUKI SATO[1]

Department of [1]Pathology, [2]Surgery Ist and [4]Surgical Pathology, Sapporo Medical University School of Medicine, Sapporo, Japan; [3]Department of Surgery, Shinsapporo Keiaikai Hospital, Sapporo, Japan; [5]Dainippon Sumitomo Pharma Co., Ltd., Osaka, Japan

Abstract. *Invasion into the matrix is one of hallmarks of malignant diseases and is the first step for tumor metastasis. Thus, analysis of the molecular mechanisms of invasion is essential to overcome tumor cell invasion. In the present study, we screened for colon carcinoma-specific genes using a cDNA microarray database of colon carcinoma tissues and normal colon tissues, and we found that fermitin family member-1 (FERMT1) is overexpressed in colon carcinoma cells. FRRMT1, FERMT2 and FERMT3 expression was investigated in colon carcinoma cells. Reverse transcription polymerase chain reaction (RT-PCR) analysis revealed that only FERMT1 had cancer cell-specific expression. Protein expression of FERMT1 was confirmed by western blotting and immunohistochemical staining. To address the molecular functions of FERMT genes in colon carcinoma cells, we established FERMT1-, FERMT2- and FERMT3-overexpressing colon carcinoma cells. FERMT1-overexpressing cells exhibited greater invasive ability than did FERMT2- and FERMT3-overexpressing cells. On the other hand, FERMT1-, FERMT2- and FERMT3-overexpressing cells exhibited enhancement of cell growth. Taken together, the results of this study indicate that FERMT1 is expressed specifically in colon carcinoma cells, and has roles in matrix invasion and cell growth. These findings indicate that FERMT1 is a potential molecular target for cancer therapy.*

Correspondence to: Yoshihiko Hirohashi and Toshihiko Torigoe, Department of Pathology, Sapporo Medical University School of Medicine, South-1 West-17, Chuo-ku, Sapporo 060-8556, Japan. Tel: +81 116138374, Fax: +81 116432310, e-mail: hirohash@sapmed.ac.jp and torigoe@sapmed.ac.jp

Key Words: Colon carcinoma, invasion, *FERMT1*, DNA microarray, fermitin family.

0250-7005/2013 $2.00+.40

Colon carcinoma is a major malignancy, with a high mortality rate. In the process of tumorigenesis, tumor cells undergo multiple steps of genetic events (1), and multiple steps are also required for the cells to obtain several different phenotypes. Tissue invasion and metastasis are hallmarks that distinguish malignant from benign diseases (2). Several classes of proteins are involved in the process of tissue invasion; however, the exact molecular mechanisms of invasion remain unclear.

Fermitin family member (*FERMT*) genes include *FERMT1*, *FERMT2* and *FERMT3*, and these genes have been reported to be mammalian homologs of the *Caenorhabditis elegans* gene (3,4). The *unc-112* gene mutant had a phenotype similar to that of *unc-52* (perlecan), *pat-2* (α-integrin) and *pat-3* (β-integrin) mutants, and *unc-112* has been described as a novel matrix-associated protein (3). In subsequent studies, *FERMT2* was found to be related to invasion in MCF-7 breast carcinoma cells (5). *FERMT1* has been reported to be overexpressed in lung carcinoma cells and colon carcinoma cells (4), and has been reported to be related to invasion of breast carcinoma cells (6). However, the molecular functions of *FERMT1* in colon carcinoma cells remain elusive.

In this study, we screened a gene expression database of carcinoma tissues to analyze the molecular mechanisms of colon carcinoma, and we isolated *FERMT1* as a gene overexpressed in colon carcinoma tissues. We then analyzed the molecular functions of *FERMT* genes in colon carcinoma cells.

Materials and Methods

Cell lines, culture, cell growth assay and gene transfer. Colon adenocarcinoma cell lines HCT116, HCT15, Colo205, SW480, CaCO2, RTK, SW48, LoVo, DLD1, HT29 and Colo320 were kind gifts from Dr. K. Imai (Sapporo, Japan), and the KM12LM cell line was a kind gift from Dr. K. Itoh (Kurume, Japan). All cell lines were

cultured in Dulbecco's Modified Eagle's Medium (DMEM) (Sigma Chemical Co., St. Louis, MO, USA) supplemented with 10% fetal bovine serum (FBS) (Life Technologies Japan, Tokyo, Japan).

For cell growth assay, 1×10^5 cells were seeded in a 6-well plate, and total cell numbers were counted every day by using Countess™ (Life Technologies).

A retrovirus system was used for gene transfer, as described previously (7). Briefly, a pMXs-puro retroviral vector was transfected into PLAT-A amphotropic packaging cells (kind gift from Dr. T. Kitamura), and then HCT116 and SW480 cells were infected with the retrovirus. Puromycin was added at 5 μg/ml for establishment of stable transformants.

Reverse transcription polymerase chain reaction (RT-PCR) analysis of FERMT genes in normal tissues and colon carcinoma cells. RT-PCR analysis was performed as described previously (8). Primer pairs used for RT-PCR analysis were 5'-GTCTGCTGAAACACAGGATTT-3' and 5'-GTTTTTCTAGTGGTTCTCCTT-3' for *FERMT1*, with an expected PCR product size of 272 base pairs (bps); 5'-CATGACATCAGAGAATCATTT-3' and 5'-ACTGGATTCTTCTTTGCTCTT-3' for *FERMT2*, with an expected PCR product size of 256 bps; 5'-AAAGTTCAAGGCCAAGCAGCT-3' and 5'-TGAAGGCCA CATTGATGTGTT-3' for *FERMT3* with an expected PCR product size of 326 bps; and 5'-ACCACAGTCCATGCCATCAC-3' and 5'-TCCACCACCCTGTTGCTGTA-3' for glyceraldehyde-3-phosphate dehydrogenase (*GAPDH*) with an expected product size of 452 bps. *GAPDH* was used as an internal control. The PCR products were visualized with ethidium bromide staining under UV light after electrophoresis on 1.2% agarose gel. Nucleotide sequences of the PCR products were confirmed by direct sequencing.

Construction of plasmids and transfection. Full-length *FERMT1*, *FRERMT2* and *FERMT3* cDNAs were amplified from cDNA of LoVo cells with PCR using KOD-Plus DNA polymerase (Toyobo, Osaka, Japan). The primer pairs were 5'-CGGGGTACCATGCTGTCATCC ACTGACTTT-3' as a forward primer and 5'-CCGCTCGAGATCCTG ACCGCCGGTCAATTT-3' as a reverse primer (underlines indicating *KpnI* and *XhoI* recognition sites, respectively) for *FERMT1*, 5'-CGGGGTACCGCCACCATGGCTCTGGACGGGATAAGG-3' as a forward primer and 5'-CCGCTCGAGCACCCAACCACTGGTA AGTTT-3' as a reverse primer for *FERMT2*, and 5'-CGGGGTACC GCCACCATGGCGGGGATGAAGACAGCC-3' as a forward primer and 5'-CCGCTCGAGGAAGGCCTCATGGCCCCCGGT-3' as a reverse primer for *FERMT3*. The PCR product was inserted into the pcDNA3.1 expression vector (Life Technologies) fused with a FLAG-tag. The cDNA sequences were confirmed by direct sequencing, and proved to be identical as reported previously (4). The inserts were then sub-cloned into a pMXs-puro retrovirus vector (kind gift from Dr. T. Kitamura, Tokyo, Japan). For the construct of protein expression, a *BglII* and *XhoI*-digested deletion mutant of *FERMT1* cDNA that was amplified by PCR using the primer pair 5'-GAAGATCTATGCT GTCATCCACTGACTTT-3' and 5'-CCGCTCGAGATCCTGACCGC CGGTCAATTT-3' (underlines indicating *BglII* and *XhoI* recognition sites, respectively) was inserted into a *BamHI* and *XhoI*-digested pQE30 (Qiagen Japan, Tokyo, Japan) vector.

FERMT1 recombinant protein production and establishment of a monoclonal antibody (mAb). A pQE30-*FERMT1* deletion mutant construct was transformed into Escherichia coli strain M15 (Qiagane Japan, Tokyo, Japan), and His6 tag-fused FERMT1 protein was induced with 1 mM Isopropyl β-D-1-thiogalactopyranoside (IPTG) for 4 h at 30°C. Cells were lysed in lysis buffer [6 M guanidine hydrochloride, 20 mM HEPES (pH 8.0), 50 mM NaCl], and recombinant FERMT1 protein was purified using Ni-NTA resin (Qiagen Japan).

The FERMT1 recombinant protein (100 μg) was used for immunization of BALB/c mice (CHARLES RIVER LABORATORIES JAPAN, INC., Yokohama, Japan) by intraperitoneal (*i.p.*) injection four times at two-week intervals. One week after the last injection, splenic cells were collected and fused with the NS-1 mouse myeloma cell line (ATCC, Manassas, VA, USA) at a 4:1 ratio. FERMT1 protein-specific hybrydomas were screened with enzyme-linked immunosorbent assay (ELISA) and western blotting using recombinant FERMT1 protein.

Immunohistochemical staining and western blotting. Immunohistochemical staining was performed with a colon carcinoma tissue microarray established from formalin-fixed surgically-resected tumor specimens of colon carcinoma at Sapporo the Medical University Hospital, as described previously (8). Anti-FERMT1 antibody was used at a 10-fold dilution with the anti-FERMT1-specific hybridoma culture supernatant. Western blotting of colon carcinoma tissues and colon carcinoma cells was performed as described previously (8). Anti-FERMT1 antibody was used at a 10-fold dilution with hybridoma culture supernatant.

Matrigel invasion assay. BD BioCoat Matrigel Invasion Chambers (Discovery Labware, Bedford, MA, USA) and polyethylene terephthalate (PET) track-etched membranes with pore sizes of 8.0 μm (Becton Dickinson, San Diego, CA, USA) were used for the invasion assay, according to the protocol of the manufacturer. HCT116- and SW480-transformant cells (2.5×10^4 cells/500 ml) were plated in the top chamber in DMEM, and culture medium with 10% FBS was used in the bottom chamber as a chemoattractant. Twenty-four hours later, cells were fixed and stained using a HEMA 3 STAT Pack (Fisher Scientific Japan, Tokyo, Japan). Cell numbers were counted on microphotographs taken in ten areas of the membrane.

Statistical analysis. In cell growth assays and invasion assays, samples were analyzed using Student's *t*-test, with $p<0.05$ conferring statistical significance.

Results

Isolation of the colon carcinoma-related gene FERMT1. We screened a gene expression database of approximately 700 normal organ tissues and about 4000 carcinoma tissues using the Affymetrix GeneChip Human Genome U133 Array Set that contains approximately 39,000 genes. One of the genes that was overexpressed in colon carcinoma tissues was shown to be *FERMT1*, a member of the *FERMT* gene family. In a previous study, *FERMT1* was shown to be overexpressed in lung carcinoma cells and colon carcinoma cells (4). FERMT1 is member of a family of highly homologous gene products including FERMT2 and FERMT3 (Figure 1A). *FERMT1*, *FERMT2* and *FERMT3* share a FERM domain and a Pleckstrin homology domain (PH) domain, which are a cytoskeletal-associated domain and phosphatidylinositol

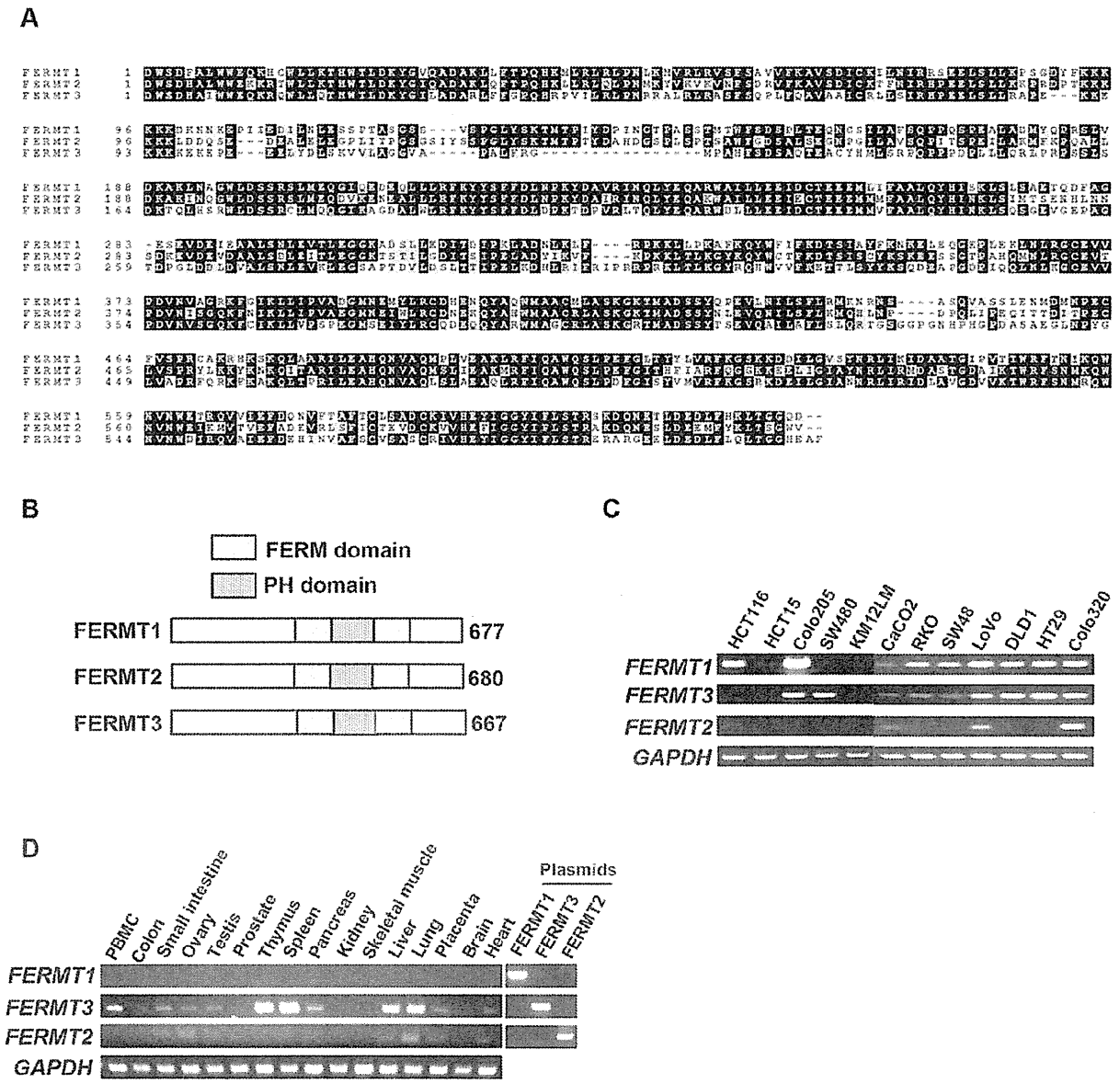

Figure 1. *Expression profiles of fermitin family member (FERMT) family genes. A: Sequence alignment of FERMT proteins. FERMT1, FERMT2 and FERMT3 amino acid sequences are shown. A black box indicates the same alignment, a gray box indicates similar alignment. B: Molecular structure of FERMT family proteins. A dotted box indicates the FERMT domain, cytoskeletal-associated domain, a lined box indicates the Pleckstrin homology domain (PH) domain, phosphatidylinositol lipid association domain. C: Reverse transcription-polymerase chain reaction (RT-PCR) of FERMT family in colon carcinoma cells. FERMT1, FERMT2 and FERMT3 expression in colon carcinoma cells was evaluated by RT-PCR. Glyceraldehyde 3-phosphate dehydrogenase (GAPDH) was used as an internal positive control. D: RT-PCR of FERMT family genes in normal organ tissues. FERMT1, FERMT2 and FERMT3 expression in normal organ tissues was evaluated by RT-PCR. FERMT1, FERMT2 and FERMT3 plasmids were used as positive controls. GAPDH was used as an internal positive control.*

lipids association domain, respectively (Figure 1B). Since *FERMT1*, *FERMT2* and *FERMT3* show high homology with each other, we evaluated the expressions of these genes in colon carcinoma cells and also in normal organ tissues by RT-PCR. *FERMT1* was expressed in 9 (75%) out of 12 colon carcinoma line cells, and *FERMT3* was expressed in 9 (75%) out of 12 colon carcinoma line cells and *FERMT2* was expressed in 3 (25%) out of 12 colon carcinoma line cells

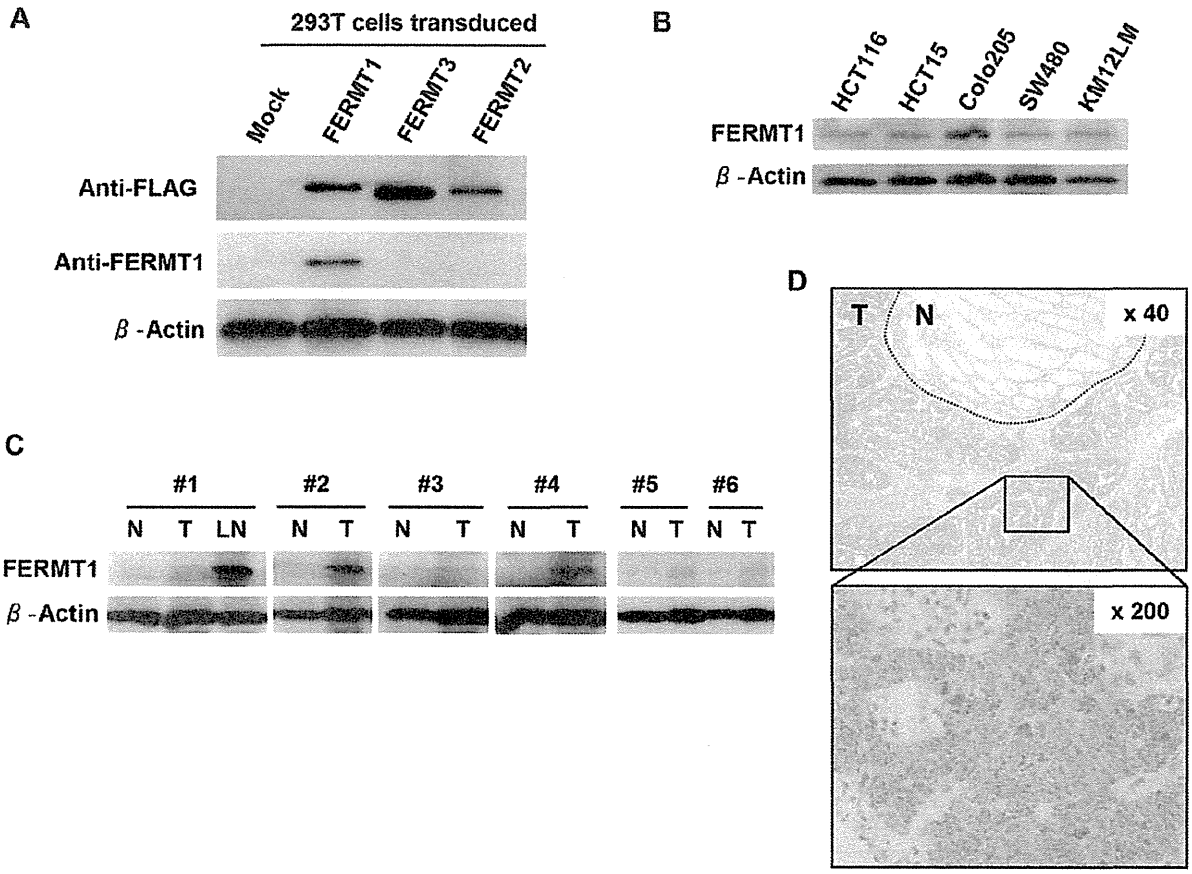

Figure 2. *Fermitin family member 1 (FERMT1) protein expression in colonic carcinomas. A: Western blotting using monoclonal antibody (mAb) against FERMT1. 293T cells were transfected with FERMT1, FERMT2 and FERMT3 plasmids. Western blotting using anti-FLAG mAb and anti-FERMT1 mAb was performed. Anti-FLAG mAb was used as a positive control. β-Actin was used as an internal positive control. B: Western blotting of colonic carcinoma cells. Western blotting using anti-FERMT1 mAb was performed. β-Actin was used as an internal positive control. C: Western blot of colon carcinoma tissues. Protein expression of FERMT1 in primary human colonic carcinoma cases (#1-#6) was evaluated by western blotting using an anti-FERMT1 mAb. T, Tumoral part of colonic carcinoma tissue; N, adjacent normal colonic mucosa tissue; LN, lymph node metastatic tissue of the corresponding case. β-Actin was used as an internal positive control. D: Immunohistochemical staining of FERMT1. Representative images of immunohistochemical staining of colonic carcinoma tissues using anti-FERMT1 mAb are shown. Brown indicates positive staining. Dotted line indicates normal colonic mucosa cells. N, Normal colon mucosa tissue; T, colonic carcinoma tissue.*

(Figure 1C). *FERMT1* was not expressed in normal organ tissues, whereas *FERMT3* and *FERMT2* were expressed ubiquitously in normal organ tissues. Only *FERMT1* exhibits colon carcinoma cell-specific expression. We therefore focused on *FERMT1* for further analysis.

Protein expression of FERMT1 in colon carcinoma cells and tissues. To address FERMT1 protein expression, we established a novel anti-FERMT1 mAb. Since FERMT1, FERMT2 and FERMT3 have similar protein structures, we evaluated the specificity of the mAb to FERMT1. FERMT1 mAb showed reactivity for 293T cells transfected with a FERMT1 expression vector, whereas it did not react to 293T cells transfected with a FERMT2 or FERMT3 vector, as shown in western blot analysis (Figure 2A), indicating that the mAb against FERMT1 mAb is specific for FERMT1. Western blot analysis revealed positive FERMT1 protein expression in all five colon carcinoma lines tested (Figure 2B).

Further evaluation of FERMT1 protein expression in primary colon carcinoma tissues was performed. Six colon carcinoma primary tumor tissues exhibited higher levels of FERMT1 protein expression than those in adjacent normal colonic mucosa tissues (Figure 2C). Of note, stronger FERMT1 protein expression was detected in tissue from lymph node metastasis of case #1 than in primary colonic tumor tissue and normal colonic mucosa of the same case.

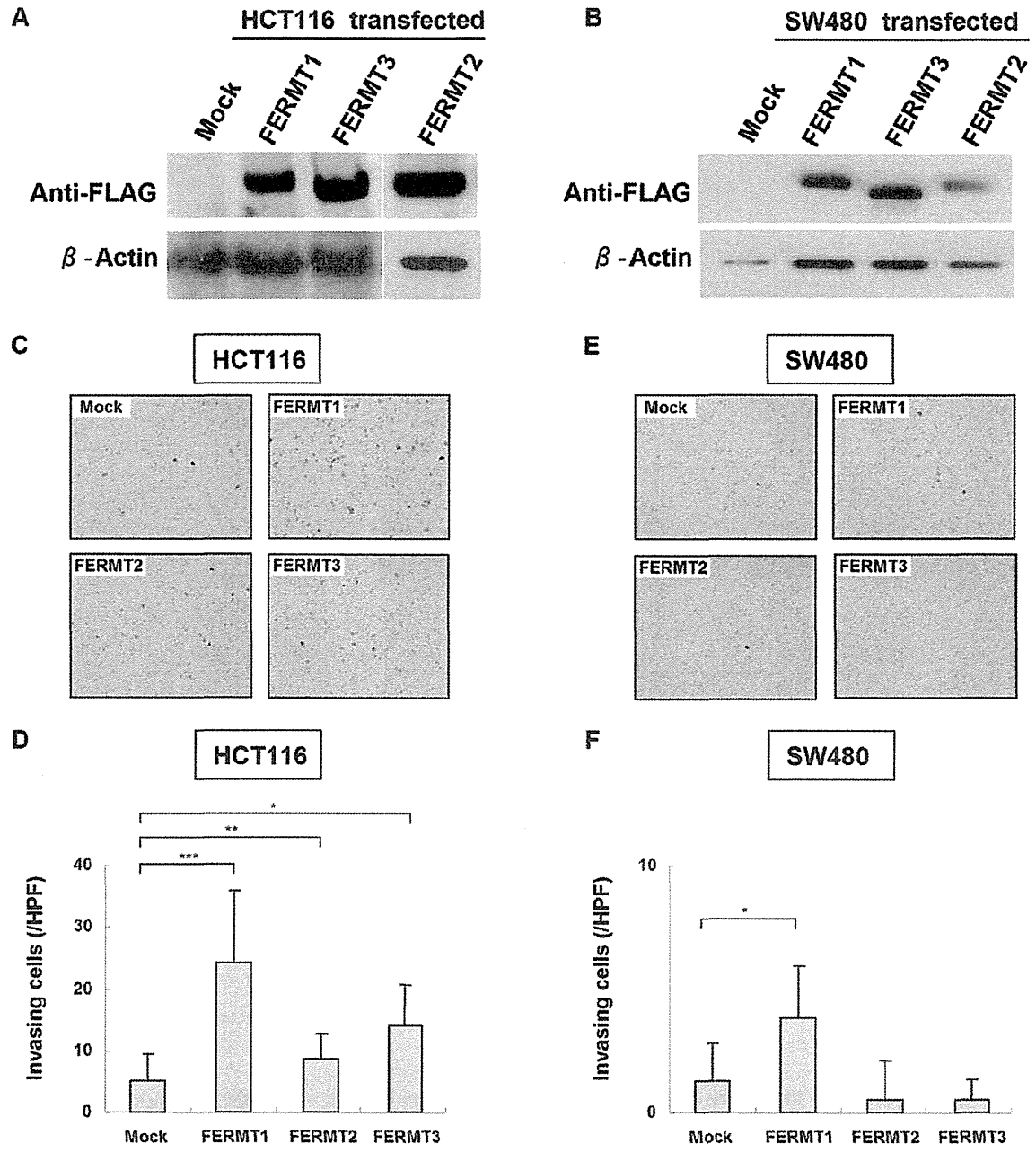

Figure 3. *Molecular function of FERMT1 in colon carcinoma cells. A: Western blotting using monoclonal antibody (mAb) to FLAG-tag. HCT116 cells were transfected with FREMT1, FERMT3, FERMT2 plasmids, and analyzed by western blot using mAb to FLAG-tag. β-Actin was used as an internal positive control. B: Western blotting using a monoclonal antibody (mAb) to FLAG-tag. SW480 cells were transfected with FREMT1, FERMT3, FERMT2 plasmids, and analyzed by western blot using a mAb to FLAG-tag. β-Actin was used as an internal positive control. C: Invasion assay of FERMT family-overexpressing HCT116 cells. Representative images of invasion assay using FERMT family cDNA-overexpressing HCT116 cells. Purple cells indicate HCT116 cells that have invaded through the Matrigel. D: Invasion assay of FERMT family-overexpressing HCT116 cells. Invading cells were counted in 10 high power fields (HPFs). Data represent means±SD. Differences between FERMT family-overexpressing HCT116 cells and mock-transfected HCT116 cells were examined for statistical significance using the Student's t-test. *p=0.03, **p=0.001, ***p<0.0001. E: Invasion assay of FERMT family-overexpressing SW480 cells. Representative images of invasion assay using FERMT family cDNA-overexpressing SW480 cells. Purple cells indicate SW480 cells that have invaded through the Matrigel. F: Invasion assay of FERMT family-overexpressing SW480 cells. Invaded cells were counted in 10 HPF. Data represent means+SD. Differences between FERMT family-overexpressing SW480 cells and mock-transfected SW480 cells were examined for statistical significance using Student's t-test. *p=0.04.*

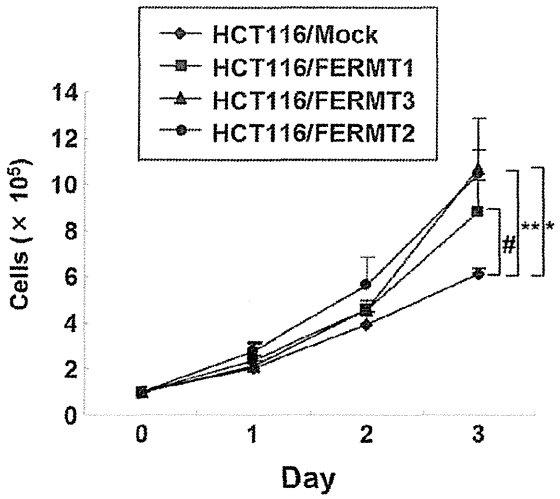

Figure 4. *Cell growth of FERMT famliy-overexpressing HCT116 cells. FERMT family cDNA-overexpressing HCT116 cells were seeded in a 6-well plate, and the cell growth rate was recorded daily. Data represent means±SD. Differences between FERMT family-overexpressing HCT116 cells and mock-transfected HCT116 cells were examined for statistical significance using Student's t-test. *p=0.015, #p=0.012, **p=0.001.*

Immunohistochemical staining of primary colonic carcinoma tissues also revealed FERMT1 protein expression in carcinoma cells but not in normal epithelial cells (Figure 2D). The positive immunohistochemical staining rate of FERMT1 protein in colon carcinoma tissues was 95% (38 out of 40 cases).

Role of FERMT1 in invasion and cell growth. Since western blot analysis revealed a high level of FERMT1 protein expression in lymph node metastasis tissue, we hypothesized that FERMT1 is related to the invasion of colonic carcinoma cells. In order to analyze the functions of *FERMT* genes, we established *FERMT1*-, *FERMT2*- and *FERMT3*-overexpressing HCT116 cells and SW480 cells. Protein expression of FERMT1, FERMT2 and FERMT3 was confirmed by western blot analysis, using an anti-FLAG antibody (Figure 3A and 3B). Invasion assays using Matrigel were performed, and FERMT1-overexpressing HCT116 cells exhibited greater invasive ability than mock vector-transformed HCT116 cells ($p<0.001$) (Figure 3C and 3D). *FERMT1*-overexpressing SW480 cells also exhibited greater invasive ability than did mock-transfected SW480 cells (Figure 3E and 3F). *FERMT2* and *FERMT3* had the ability to enhance the invasion of HCT116 cells, whereas they had no effect on SW480 cells. Cell growth ability was evaluated by a cell growth assay. *FERMT1*-, *FERMT2*- and *FERMT3*-overexpressing HCT116 cells showed greater growth *in vitro* than non-transfected cells, indicating that *FERMT1*, *FERMT2* and *FERMT3* have roles in cell growth (Figure 4).

Discussion

During cancer progression, cells gain multiple abilities allowing them to become malignant cells. Malignant diseases are defined by invasion into adjacent organs and distant metastasis, and invasion is thus a prominent ability of malignant cells. In this study, we identified *FERMT1* as a colon carcinoma-related gene by screening of a gene database. *FERMT1* was reported to be overexpressed in lung carcinoma cells and colonic carcinoma cells (4). However, the molecular functions of *FERMT1* in colonic carcinoma cells have not been elucidated. In another study, *FERMT1* was shown to be overexpressed in lung metastasis of breast carcinoma (9). The same research group reported that *FERMT1* has a role in epithelial mesenchymal transition through activation of transforming growth factor-β (TGFβ) signaling (6). However, the molecular functions of *FERMT1* have remained elusive, and we therefore analyzed *FERMT1* function in colon carcinoma cells.

FERMT1 has 80% homology with *FERMT2* and 72% homology with *FERMT3*. The three molecules have similar domain structures (Figure 1B), suggesting similar molecular functions. However, the expression profiles of *FERMT1*, *FERMT2* and *FERMT3* in normal organ tissues exhibited significant differences, and only *FERMT1* showed carcinoma cell-specific expression. In this study, we did not address the expression of *FERMT1* in skin tissue; however, previous studies showed that *FERMT1* is expressed in skin keratinocytes and that gene mutation in *FERMT1* is related to Kindler syndrome (10-12). *FERMT2* was shown to have invasion ability in MCF7 breast carcinoma cells (5). *FERMT3* was reported to be expressed in leukocytes and to have a role in the activation of integrin signals (13, 14); however, there has been no report describing the relationship between *FERMT3* and invasion. In our study, *FERMT1*, *FERMT2* and *FRMT3* were all shown to have roles in invasion, indicating that they may have similar functions. *FERMT1* and *FERMT2* have been reported to share some molecular functions in skin keratinocytes (15, 16). These observations indicate that *FERMT1*, *FERMT2* and *FERMT3* may have similar molecular functions and that the difference in expression defines the role of each molecule. Of note, *FERMT1* is ectopically and specifically overexpressed in carcinoma cells and *FERMT1* is thus the most suitable target for future cancer therapy.

In summary, to our knowledge this is the first report on *FERMT1* functions in colon carcinoma cells. While *FERMT1*, *FERMT2* and *FERMT3* are expressed in colon carcinoma cells, only *FERMT1* exhibites cancer cell-specific expression. FERMT1 also has a role in invasion and growth of colonic carcinoma cells. The results indicate that *FERMT1* is a possible target for cancer therapy.